Sedimentary features and palaeogeography of the youngest deposits in the Bohemian Cretaceous Basin (Merboltice Formation, Santonian)

Jaroslav Valečka

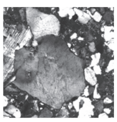

A relic of the Merboltice Formation of the Santonian age, up to 200 m thick, is preserved over an area of 800 km^2 in a deeply buried block within the Tertiary Ohře Rift, in the north-western part of the Bohemian Cretaceous Basin. The Formation represents the youngest deposits preserved in this basin. The Formation was studied in detail at eight large outcrops and in three boreholes. It consists of a succession of several centimetres- to several metres-thick sandstone beds, with sharp to erosive contacts, that typically grade upward into dark mudstones. Thin, sharply bounded intercalations of greenish, light grey mudstones are found rarely between the sandstone beds. Facies analysis performed here suggests that these beds were deposited from gravity flows, mostly as "cogenetic turbidite-debrite beds", or, less frequently, as deposits either from cohesive debris-flows or turbidity currents. Most of the beds record vanning of a cohesive flow and its transition into a turbidity current. The predominance of debrites allowed for a higher clay content in the sandstones (6–15%, occasionally up to 17.5%). The intercalated mudstones reflect periods of quiet suspension settling between the deposition from gravity flows. Petrographic analysis showed a uniform composition of the sandstones, falling into a very narrow field of subarcoses. Feldspar contents with a large predominance of K-feldspars, most of them only slightly altered, range from 6–15%. Granitoids are present along with stable quartzites and cherts, in the rock fragments. The Merboltice Fm., which formed during the regressive phase under the influence of gravity flows, represents exceptional facies, which has no counterpart in any of the Cretaceous basins in the Bohemian Massif. Its formation was enabled by an accelerated uplift of the source area north of the Lusatian Fault at the basin margin and erosion of the uplifted sediments, granitoids, and, to a lesser extent, metamorphites. Large amounts of detritus accumulated near the coast of the basin and were transported by gravity flows to a distance of up to ~ 50 km. It is hypothesized here that these flows were mainly initiated by increased seismic activity on the Lusatian Fault, whereas other faults of the Elbe Fault System appeared inactive. The activity of gravity currents may have been facilitated by an increased slope of the basin margin near the Lusatian Fault. The gravity flows could also have been triggered by storms or by the collapse of thick sand deposits (delta) near the river mouths. Structures attributable to hyperpycnal currents were not detected. The frequency of gravity flows made sedimentation of mudstone deposits from suspension a subordinate process, in marked contrast to the underlying Březno Formation (Coniacian). • Key words: Bohemian Cretaceous Basin, Middle Europe, Santonian, subarcoses, mudstones, gravity flows, trace fossils, palaeogeography.

Valečka, J. 2024. Sedimentary features and palaeogeography of the youngest deposits in the Bohemian Cretaceous Basin (Merboltice Formation, Santonian). *Bulletin of Geosciences 99*(*4*), 297–322 (16 figures, 2 tables). Czech Geological Survey, Prague. ISSN 1214-1119. Manuscript received December 20, 2023; accepted in revised form October 29, 2024; published online December 31, 2024; issued December 31, 2024.

Jaroslav Valečka, Czech Geological Survey, Klárov 3/131, Praha 1, 118 00, Czech Republic; jaroslav.valecka@geology.cz

The youngest deposits of the Bohemian Cretaceous Basin, classified by Čech *et al.* (1980) as the Merboltice Formation of the Santonian age, are preserved only in the northern part of the basin, in the central and eastern parts of the České Středohoří Mts., in the vicinity of Ústí nad Labem and Děčín, Czechia (Fig. 1B). The formation, composed of sandstones with subordinate mudstones, was originally classified as Tertiary in age due to scarcity of fossils. The previous research focused mainly on the chrono- or lithostratigraphy of the formation. Except for a few localized studies, petrological, sedimentological or palaeogeographical analyses have not yet been published to date. Petrological data (grain size, contents and composition of the clay fraction) were reported only from the Zálezly sand pit (now abandoned, south of Ústí nad Labem; Gabriel 1984), two abandoned sand pits near Skorotice and a shallow borehole near Malé Chvojno, in the northern surroundings of Ústí nad Labem (Zelenka 1980). A sedimentological analysis was carried out only at the type locality in the Merboltice quarry (unpublished report by Valečka & Slavík 1985) and suggests that the Merboltice Formation exhibits a relatively

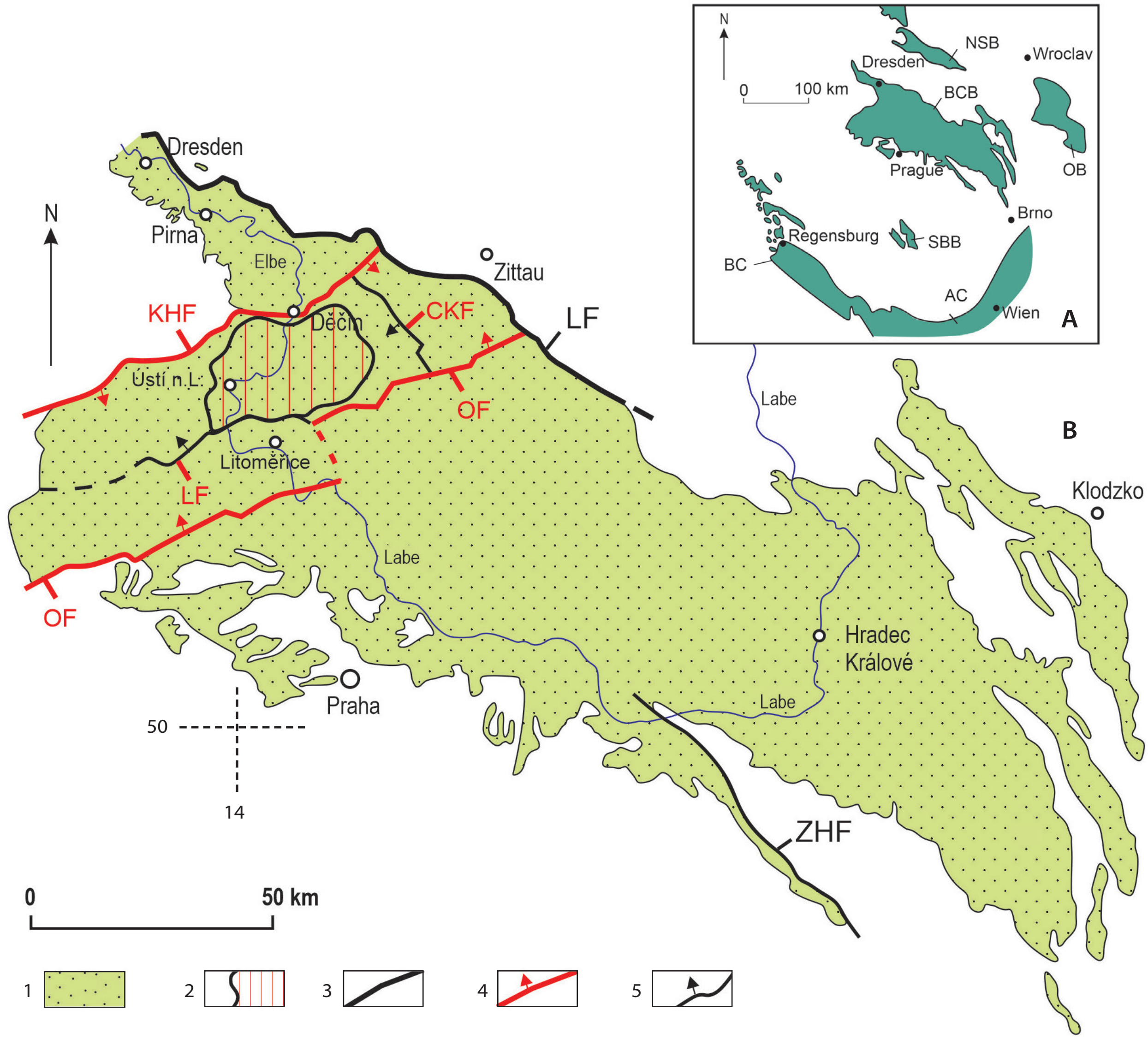

Figure 1. A – Late Cretaceous basins within the Bohemian Massif (adapted from Valečka & Skoček 1991). Abbreviations: AC – autochthonous Cretaceous on the southern and south-eastern slopes of the Bohemian Massif; BC – Bavarian Cretaceous Basin (Regensburg Basin or Regensburg Gulf); BCB – Bohemian Cretaceous Basin; NSB – North Sudetic Basin; OB – Opole Basin; SBB – South Bohemian Basin. • B – position of the Merboltice Formation in the Bohemian Cretaceous Basin. Legend: 1 – Bohemian Cretaceous Basin; 2 – Merboltice Fm. area; 3 – important faults (LF – Lusatian Fault, ZHF – Železné hory Mts. Fault); 4 – boundary faults of the Ohře Rift; (KHF – Krušné hory Mts. Fault, OF – Ohře Fault; 5 – faults within the Ohře Rift (LF – Litoměřice Fault, CKF – Česká Kamenice Fault).

low mineralogical maturity due to an elevated feldspar content (up to 12–15%) and sedimentary structures that are indicative of deposition from density flows. These features make the Merboltice Formation unique in the Bohemian Cretaceous Basin and among all Upper Cretaceous basins located in the Bohemian Massif (Fig. 1A, see below Provenance). The present study focuses on sedimentological, petrographical and palaeogeographical analysis of sections across the entire erosional relic of the Merboltice Formation with the aim to interpret the depositional conditions of this unique succession.

Geological and tectonic setting

The Merboltice Formation covers the total area of *ca.* 800 km^2 in discontinuous relics in the vicinity of Ústí nad Labem. The area is situated within the Ohře Rift, Tertiary in origin. This area of occurrence is located in the deepest part of the rift and is bounded by Litoměřice and Česká Kamenice faults (Fig. 1B). The area is structurally the lowest part of the Bohemian Cretaceous Basin, with the base of basin fill located at −150 m to −650 m below the sea level. The Merboltice Formation forms the uppermost part of the ~ 1 km thick basin fill (Fig. 2) and consists of a number of erosional relics separated by deep valleys cut into the underlying Březno Formation (Fig. 3). The underlying Březno Formation, Coniacian in age, is 230 m to ~ 300 m thick and contains flysch-like facies (in the works of Czech authors called as "flyschoid facies") in its uppermost part. In several localities, the Merboltice sandstones are covered with relics of Tertiary fluvial deposits consisting of medium- to coarse-grained sandstones and conglomerates, often cross-bedded, strongly silicified and including claystone layers and Palaeogene flora (Domácí 1976, Valečka 1999, Váně 2001, Valečka & Valigurský 2003, Malý *et al.* 2006). The extent of these deposits exceeds 1 km^2 at only a few localities, the largest occurrence being northwest of Česká Lípa. Large areas of the Merboltice Formation are covered by a Tertiary volcanosedimentary complex, up to ~ 350 m thick (Fig. 3).

The Merboltice Formation formed in a sedimentary basin, which, according to Valečka (2020), had the character of a basin on a passive continental margin. Uličný (2001) and Uličný *et al.* (2009) considered this basin to be a strike-slip or transtensional basin. The detailed tectonic setting of the basin remains debated, but the reactivation of basement faults during the late Cretaceous was likely affected by a compressional event related to the convergence of Iberia and Europe (Voigt *et al.* 2021). This compression phase led to shortening of the basement accompanied by inversion movements in the existing basins and to uplift of basement blocks (anticlines). At the edge of the European Platform, the Krkonoše-Jizera Unit ("Anticlinal zone") was uplifted simultaneously with the formation of the Bohemian Cretaceous Basin (Voigt 2009). This block, called West Sudetic Island in palaeogeographic reconstructions (*e.g.* Tröger 1967, Klein *et al.* 1979, Valečka 1989, Uličný *et al.* 2009) was part of large platform basins in the Late Jurassic (Valečka 2019) and, according to some opinions (Voigt 2009), also in the Early Cretaceous. Movements of the aforementioned block and movements in the adjacent part of the basin were influenced by faults belonging to the Elbe Fault System *sensu* Scheck *et al.* (2002). Of these, the most significant faults were the Intra-Sudetic and Lusatian Fault that bounded the rising block of the West Sudetes (Voigt 2009). Within the basin, at least in some phases of sedimentation, other Elbe Fault System faults, *e.g.* the Mid-Saxonian Fault, were active (see below). For the Bohemian Cretaceous Basin, the Lusatian Fault was primarily important as an active tectonic boundary of the main source area of coarse clastics – the West Sudetic Island – situated at the NNW margin of the basin. The clastic material came from eroded Permian, Jurassic, Lower Cretaceous? and Upper Cretaceous sediments, granitoids of the Krkonoše-Jizera and Lusatian granitoid massifs and the remnants of their metamorphic mantle.

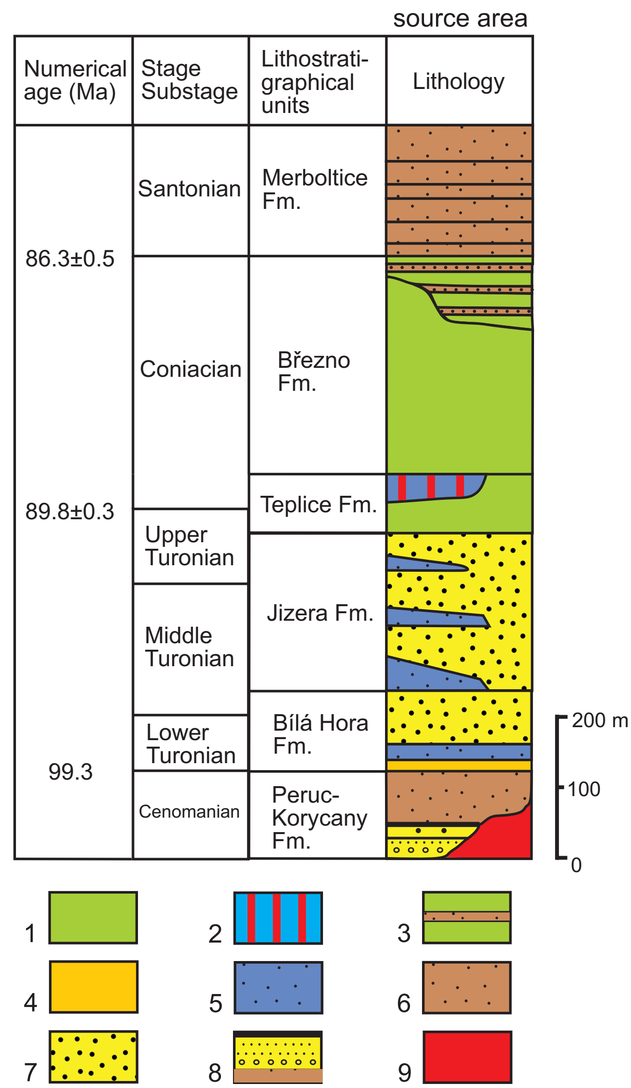

Figure 2. Simplified stratigraphic and lithologic chart of the Upper Cretaceous in the České Středohoří Mts. (numerical age is given according to the international chronostratigraphic chart 2023/2024). Legend: 1 – calcareous claystones, marlstones, in the Teplice Fm. with limestone layers; 2 – marlstones with layers of hard silicified limestones; 3 – calcareous claystones and marlstones with thin fine-grained sandstone intercalations, flysch-like facies (so-called flyschoid facies); 4 – spiculitic marlstones and spongolites; 5 – calcareous fine-grained sandstones; 6 – fine- to medium-grained clayey or quartzose sandstones, in the Merboltice Fm. fine- to medium-grained subarcoses; 7 – medium to coarse-grained quartzose sandstones; 8 – cyclic alternation of fluvial conglomerates, sandstones and dark claystones; 9 – Cretaceous basement (metamorphites, granitoids, Permo-Carboniferous sediments and volcanites).

Sandy and conglomeratic detritus accumulated in the vicinity of the Lusatian Fault, in a rapidly subsiding zone situated asymmetrically in the basinal north-eastern wing (Tröger 1967, Klein *et al.* 1979, Valečka 1989). During phases when the input of coarse detritus exceeded the accommodation in the subsiding zone, progradation occurred towards the basin axis, up to a distance of ~ 50 km.

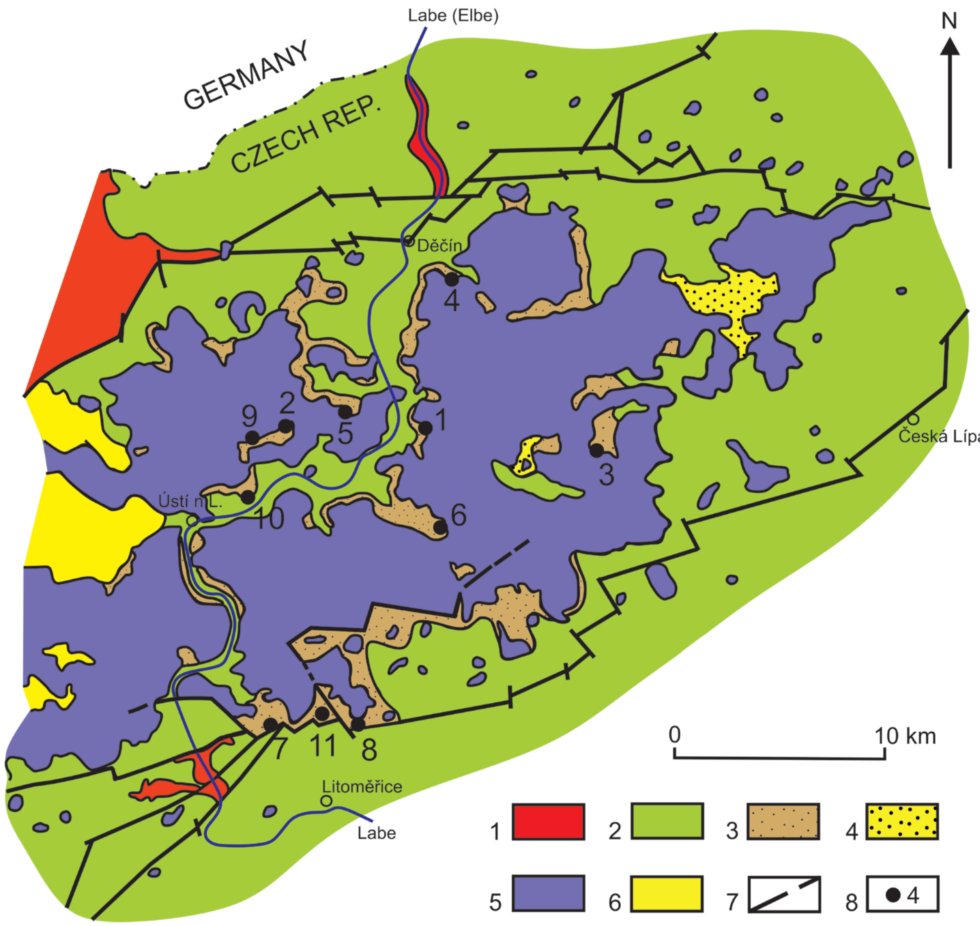

Figure 3. Geological map of the central and eastern part of the České Středohoří Mts. and vicinity. Legend: 1 – crystalline complex; Upper Cretaceous: 2 – sediments of the Cenomanian, Turonian and Coniacian (Peruc-Korycany Formation to Březno Formation); 3 – Merboltice Formation (Santonian); Tertiary: 4 – Palaeogene fluviatile sediments; 5 – Tertiary volcanosedimentary complex of the České Středohoří Mts.; 6 – North Bohemian Coal Basin; 7 – faults; 8 – localities with the sections in Figs 7 and 8.

The extent of these bodies was also influenced by synsedimentary activity of other faults (*e.g.* the Mid-Saxonian Fault) bordering to the SW rapidly subsiding zone near Lusatian Fault. The activity of the Mid-Saxonian Fault is indicated by isopachs of rapidly decreasing thickness of the Jizera Formation, concentrated in a very narrow NW–SE trending zone, running conformably with the fault (Valečka 1989).

Geological mapping and numerous deep drill holes (Tröger 1967, 1969; Valečka 1979, 1989; Klein *et al.* 1979; Coubal *et al.* 2018) suggest that the maximum thicknesses of marine lithostratigraphic units, achieved in the vicinity of the Lusatian Fault are approximately 115 m in the Korycany Member, 135 m in the Bílá hora Fm., 420 m in the Jizera Fm., 130 m in the Teplice Fm. and 500 m in the Březno Fm. The maximum preserved thickness of the basin fill, excluding the Merboltice Formation, is ~ 1.2 km. Subsidence analysis is available only for the Lower Turonian depocentre and suggests total subsidence of 158 m/Myr, of which 92 m/Myr is attributed to tectonic subsidence (Laurin *et al.* 2023). Isopach maps for the Turonian through Coniacian (Laurin & Uličný 2004, Uličný *et al.* 2009) suggest increasing asymmetry of the basin fill, with accelerated subsidence in the vicinity of the Lusatian Fault, towards the Coniacian, possibly extending to the Santonian.

Stratigraphic position of the Merboltice Formation

The extremely rare occurrence of fossils influenced the stratigraphic classification of the Merboltice Fm. One of the first authors who commented on the stratigraphy of the Merboltice sandstones was Krejčí (1869), who studied them in the vicinity of Litoměřice. Krejčí stated that “some circumstances indicate that they belong to the Chlomek beds”, *i.e.* to the youngest sediments of the Bohemian Cretaceous Basin. Maps of the České Středohoří Mts. (scale 1:25,000 with explanatory notes), published by Hibsch and collaborators between 1897 and 1930, classified these beds as "Oligocene Sand und Sandstein". The same attribution appeared in the map sheet of Česká Kamenice (Hibsch 1927). Zahálka (1914) also considered these sandstones as Oligocene in age. Similarly, Hibsch (1924) marked these beds as Oligocene sands (Oligozäner Sand) on his map of the České Středohoří Mts. at the scale of 1:100,000. Only at the end of his research did Hibsch (1930a, b) reclassified the Merboltice sandstones as a Cretaceous formation. The main reason for this update was the finding of Cretaceous fauna in sandstones in the southern surroundings of Česká Kamenice, especially in the pit in Markvartice described by Andert (1929, 1934) and Prinz (1930). Later mapping and evaluation of deep boreholes,

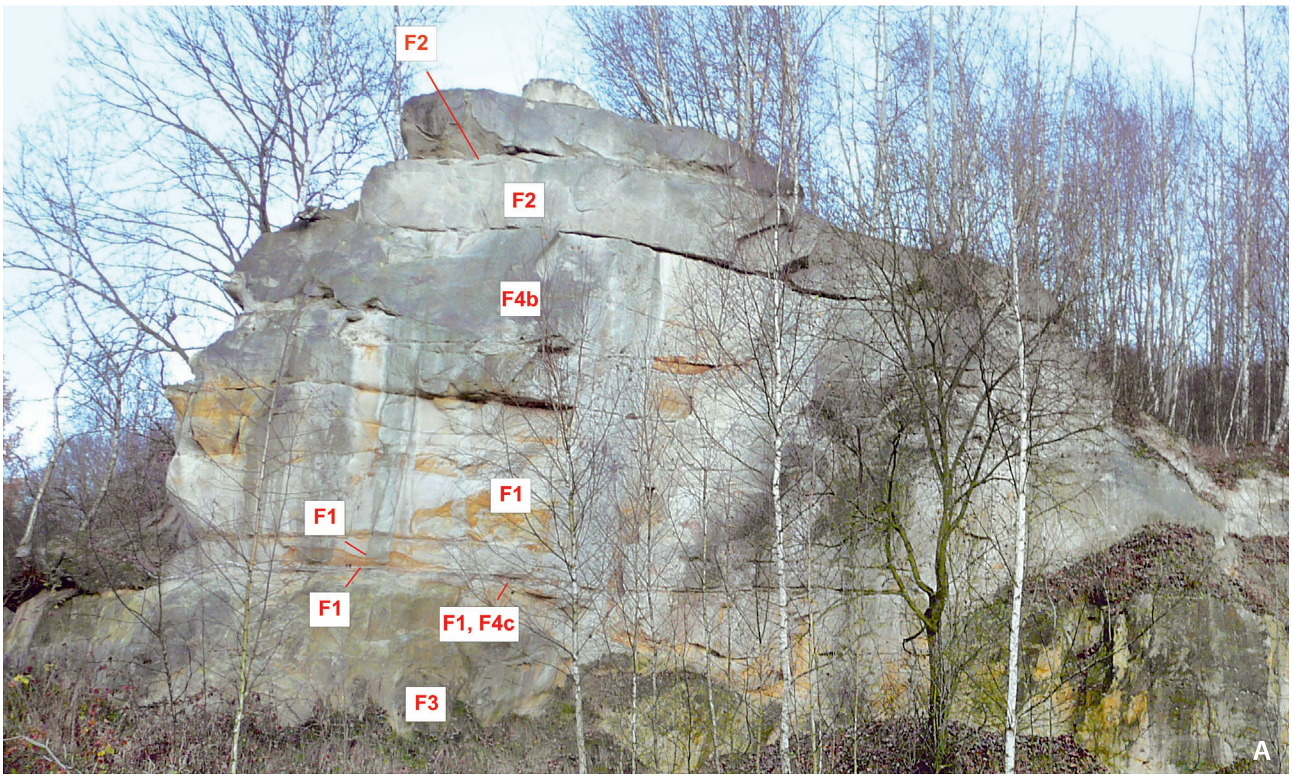

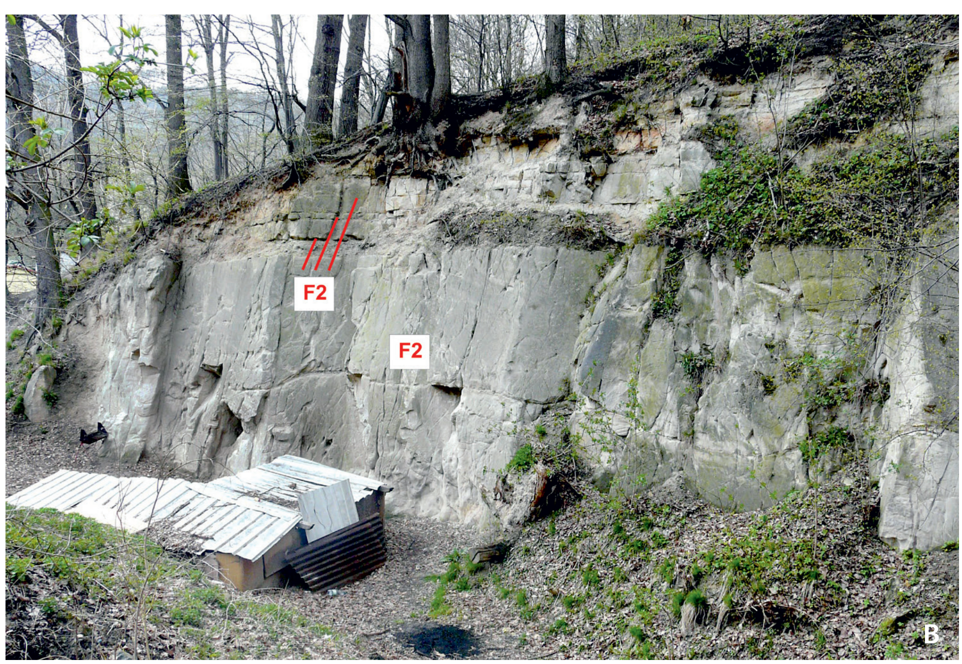

Figure 4. Studied sections in Merboltice Fm. • A – section 6, abandoned quarry in the village of Zubrnice. • B – section 9, abandoned quarry near the Ryjice village.

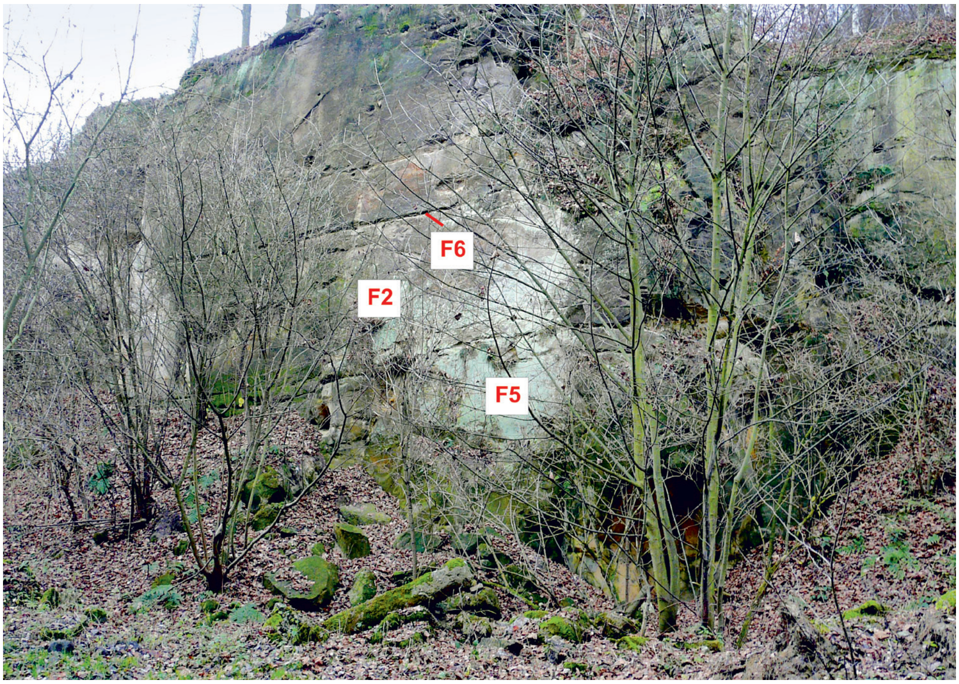

Figure 5. Section 4, abandoned quarry in the village of Březiny.

however, resulted in attribution of the sandstones in the southern surroundings of Česká Kamenice, including the sandpit in Markvartice, to the older, Březno Formation. In this area, the sandstones form bodies, several metres to tens of metres thick, embedded in calcareous mudstones. Their attribution to the Březno Formation is also supported by the discovery of an involute form of *Inoceramus* by Prinz (1930) in the sandpit in Markvartice. The *Inoceramus* specimen was determined as *Inoceramus involutus koeneni* Müller, 1887 (Andert 1929, p. 66, footnote) and later illustrated (Andert 1934, tab. 8, figs 2, 3). According to personal communication with S. Čech, it is an

Figure 6. Studied sections in Merboltice Fm. • A – middle part of section 2 in the abandoned quarry near the village of Mírkov. • B – section 10 in the abandoned quarry near the Krásné Březno village. • C – section 11 Hibsch's cave (Hibschova jeskyně) near the village Skalice, the arrow indicates the upper surface of the thick graded bed (Facies 5) in the lower part of the section.

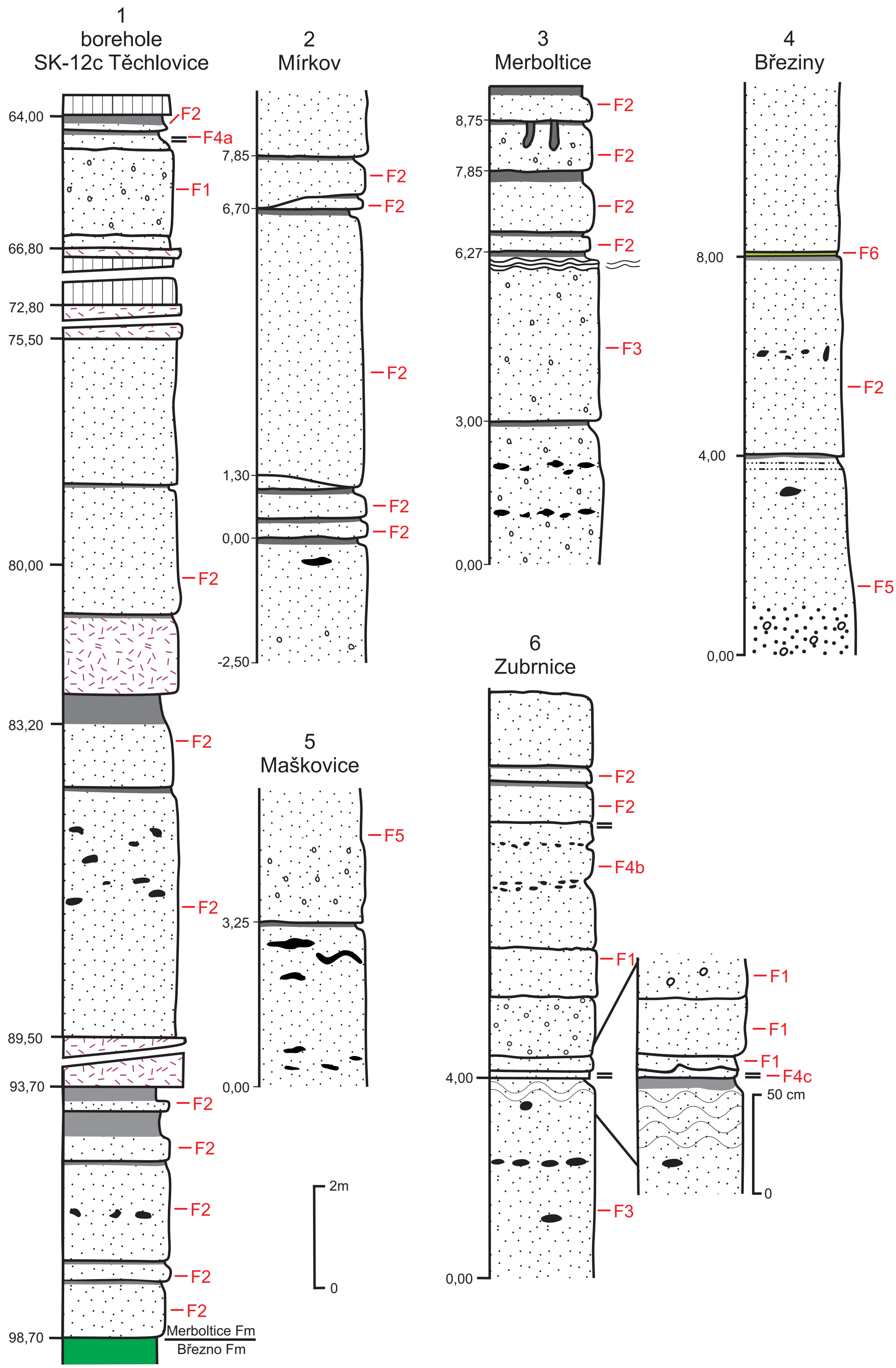

Figure 7. Structural and textural features of the Merboltice Fm. in sections 1 to 6. Explanations are in Figure 8.

involute form of an inoceramid, which is typical for the middle part of the Březno Formation. It is thus paradoxical that Hibsch reclassified the Merboltice Formation as Cretaceous on the basis of fauna from the older, Coniacian sandstones. The first real evidence of the Cretaceous age of the Merboltice Formation was provided by the discovery of the *Inoceramus* species in a quarry in Merboltice in 1959 (Fig. 15C), published by Soukup (1963), who classified the Merboltice sandstones as Lower Senonian. Klein & Soukup (1963) stated that "in the sandy facies of the České Středohoří Mts. the Upper Emscher beds, namely the *Inoceramus undulatoplicatus* and *Inoceramus cordiformis* zones, are probably represented". Further confirmation of the Cretaceous age was also provided by the findings of Cretaceous flora at the Mojžíř locality (near the section 10 in Fig. 8). At this site, Macák (1966) found flora from which Č. Bůžek identified the species *Sequoia reichenbachi* Gein. and *Myrtophyllum augusta* (Vel.). of Cretaceous age. Zelenka (1980) also mentioned the occurrence of fragments of agglutinated foraminifera of genera *Hyperammina* and *Pernerina* (determined by J. Hercogová) characteristic of shallow-marine environments. In this case, however, it may also be a redeposition from older Cretaceous deposits. Soukup (1956) concluded on the basis of inoceramids in the mudstones below the Merboltice sandstones that the "palaeontologically sterile sandstone series" above the mudstones belongs to the higher part of the Coniacian and extends to the Coniacian–Santonian boundary. Later, he states that it very probably belongs to the lower Santonian (Soukup 1968). Macák & Müller (1963, 1968) identified the species *Inoceramus subquadratus* Schlüter, 1887, *Inoceramus cycloides* Wegner, 1905 and *Inoceramus pachti* Arkhangelsky, 1912 in the calcareous claystones beneath the Merboltice sandstone and assigned the Merboltice Fm. to the Santonian *Inoceramus undulatoplicatus* Zone. Čech *et al*. (1980) defined the Merboltice Formation as a sandstone-dominated, regressive sequence of Santonian age. They defined a section in an abandoned quarry in Merboltice southeast of Děčín (Fig. 3, section 3 in Fig. 7) as the stratotype locality. The placement of the strata into the Santonian is supported by recent revisions of the ammonite and inoceramid fauna and the findings of nannofossil associations at localities in the western part of the České Středohoří Mts. in the vicinity of Ústí nad Labem. At the locality near Prackovice between the towns Ústí nad Labem and Litoměřice and in the borehole TH-29 Strážky near Ústí nad Labem, the occurrence of the highest Coniacian index fossils, namely the ammonite *Texanites pseudotexanus* (de Grossouvre, 1894) and the inoceramid *Magadiceramus crenelatus* (Seitz, 1970), was confirmed in marlstones in the uppermost 25 m of the Březno Formation (Svobodová *et al*. 2014). At the localities near Prackovice, the youngest nannofossil association in the Bohemian Cretaceous Basin was found in these marlstones, which places them in the uppermost Coniacian or in the Coniacian–Santonian boundary interval (Švábenická *et al*. 2016).

Methods

The Merboltice Formation was studied in eight sections in old quarries and sand pits and in three borehole cores (Figs 3; 4A, B; 5; 6A–C; 7; 8). These are the only sections of this formation in which the textural and structural characteristics of the individual sandstones beds and their successions can be studied. Between two and twelve individual beds were superimposed in the studied sections. Forty-four samples were taken from the sections for microscopic study. The quantity of individual components in the thin sections (quartz, feldspars, micas, rock fragments, mud, *etc.*) was determined using comparative charts. Two samples of mudstones were analysed for their $CaCO_3$ contents using the titration method in the laboratories of the Czech Geological Survey. The microphotographs were taken using the NIS-elements AR 2130 software. Seven samples from the type locality Merboltice, two samples from a borehole Úc-2 Hlinná (section 7 in Fig. 8), two samples from borehole Úd-5 Pohořany (near the section 11, Fig. 8) and six samples from localities in the Ústí nad Labem area were analysed for heavy mineral associations by Slavík (1988, the Merboltice section) and M. Fassová from Czech Geological Survey. Heavy minerals were separated from the size fraction below 0.25 mm. The number of grains analysed for a single sample ranged between 300 and 500 increasing to around 740 in the case of the Merboltice section. The heavy mineral concentrates were studied in stereoscopic and polarizing microscopes. A set of immersion liquids was used to study the transparent grains. Trace fossils descriptions are based on eight findings by the author of this paper and six samples that are deposited in the Municipal Museum of Ústí nad Labem.

Figure 8. Structural and textural features of the Merboltice Fm. in sections 7 to 11. Legend: 1 – coarse-grained sandstones with floating quartz pebbles; 2 – coarse-grained sandstones; 3 – fine to medium-grained sandstones with floating quartz pebbles; 4 – fine to medium-grained sandstones; 5 – silty-clayey fine-grained sandstones; 6 – dark mudstones; 7 – greenish grey claystones; 8 – violet-red or multicoloured mudstones; 9 – calcareous claystones; 10 – wavy lamination; 11 – horizontal lamination; 12 – mudclasts; 13 – burrows filled with mudstone; 14 – neovolcanites; 15 – interval without core; 16 – the facies described in Facies analysis.

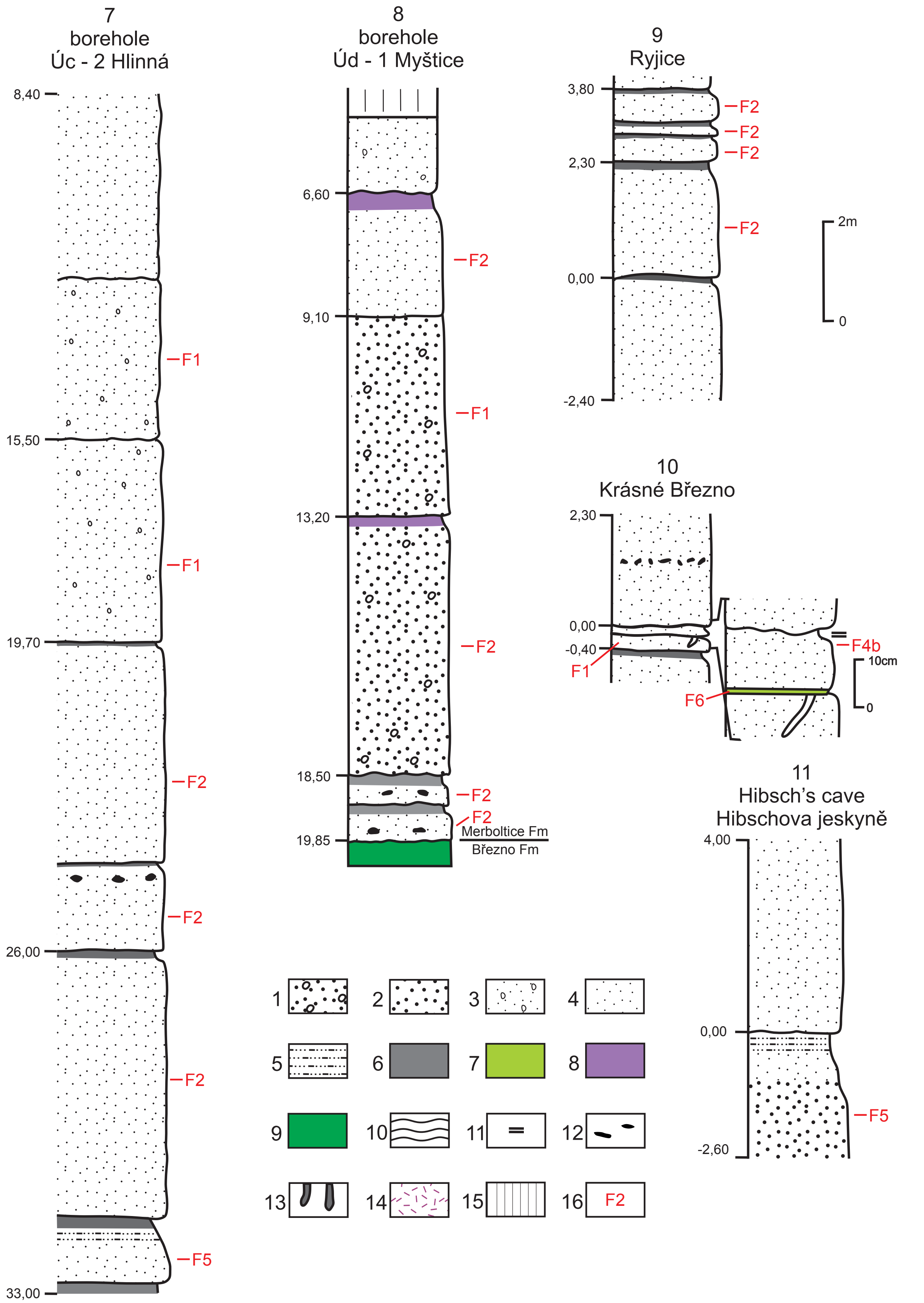
7
borehole
Úc - 2 Hlinná
8,40
15,50
19,70
26,00
33,00
F1
F1
F2
F2
F2
F5
8
borehole
Úd - 1 Myštice
6,60
9,10
13,20
18,50
19,85
F2
F1
F2
F2
F2
Merboltice Fm
Březno Fm
9
Ryjice
3,80
2,30
0,00
-2,40
F2
F2
F2
F2
2m
0
10
Krásné Březno
2,30
0,00
-0,40
F1
F6
F4b
10cm
0
11
Hibsch's cave
Hibschova jeskyně
4,00
0,00
-2,60
F5
1
2
3
4
5
6
7
8
9
10
11
12
13
14
15
16
F2

Results

Facies analysis of the Merboltice Formation

The Merboltice Fm. is characterized by the dominance of massive, grain-supported, structureless, ungraded sandstone beds that reach considerable thickness, very often in metres with maxima around 5 m. The ungraded sandstones generally make up almost the entire thickness of the beds except for their uppermost part. Some sandstones are ungraded throughout their thickness. Beds with multiple structures (divisions) of the standard Bouma (1962) sequence are scarce. The observed features suggest sedimentation from gravity flows as discussed in detail below. Papers dealing with deposition from gravity flows (notably Middleton & Hampton 1973; Lowe 1982; Mutti 1992; Shanmugan 1996, 1997, 2000, 2002; Mulder & Alexander 2001; Amy & Talling 2006, *etc.*) emphasized the sediment support mechanisms which enabled the formation of gravity flows, investigated the rheological and dynamic properties of sediment-water mixtures, and interpreted structural intervals in relation to the nature of flow. The resulting terminologies for cohesive debris and turbidite flow types and corresponding deposits, and for the relationship between structures and corresponding flow type, are not uniform (*cf.* Shanmugam 2002). In this paper the author uses the terminology of Talling *et al.* (2012, 2013), who inferred the classification of flows and their deposits from features that are visible in outcrop or core and are therefore comparable to the material of this study and that is for our aim advantageous. Talling *et al.* (2012, 2013) also detailed the standard Bouma sequence and inferred depositional processes. The small extent of outcrops of the Merboltice Formation does not allow long-distance monitoring of structural changes within individual beds. It is therefore not possible to detect changes in the structure and grain size influenced by downflow transformation (Amy *et al.* 2005, Talling *et al.* 2007) and thus to establish facies tracts *sensu* Mutti (1992), Talling *et al.* (2012, 2013) or Malgesini *et al.* (2015). The lateral stability of the beds was variable as evident from erosional truncation of two beds, 0.3 m thick, observed in the section 2 Mírkov (Fig. 7). In the sections examined in this study, 45 complete beds with both boundaries were observed in addition to 21 incomplete beds with missing lower or upper boundaries. Structural and textural analysis of the complete and some incomplete beds made it possible to distinguish six lithofacies (Figs 7, 8) and to interpret the sediment transport mechanism.

Facies 1. – Description: Nine beds in sections 1, 6, 7, 8 and 10, from 0.25 m to 4.2 m thick; the beds consist of massive, structureless, ungraded grain-supported fine- to medium-grained (in one bed coarse-grained) sandstone with clay matrix between 8% and 12%; floating (dispersed) very coarse quartz grains and small quartz pebbles up to 1.1 cm in diameter occur in five beds that are 1.85–4.2 m thick; the thickness of four beds without floating very coarse quartz grains or quartz pebbles is 0.25–1.00 m.

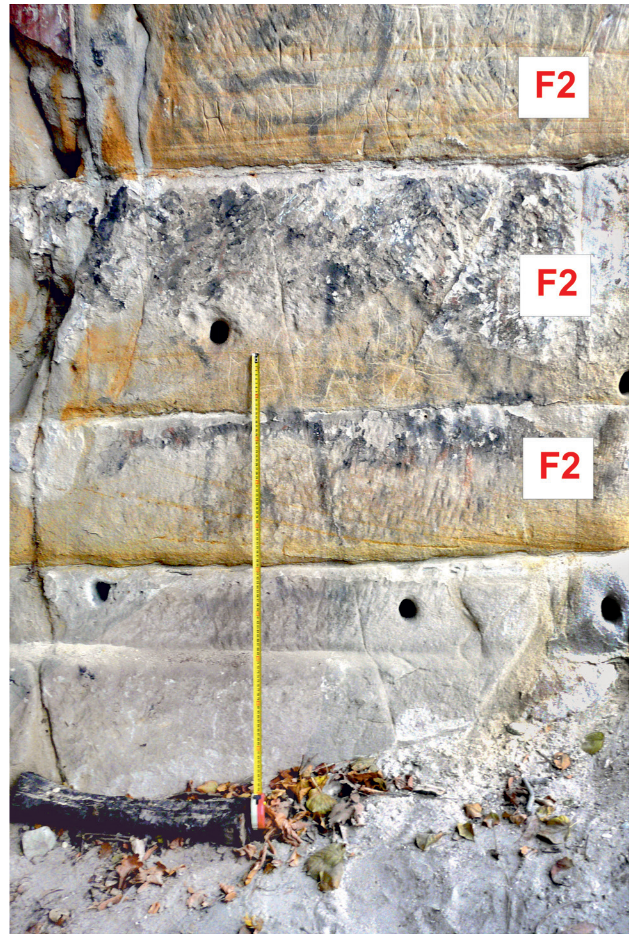

Figure 9. Superimposed beds with thin mudstone layer in the uppermost bed part (Facies 2), section 2, abandoned quarry near the Mírkov village. Artificially carved holes in the sandstone were used for wooden pins. Scale bar is 1 m.

Interpretation: Facies 1 correspond to the interval TA of Talling *et al.* (2012) (subfacies Cs6 of Talling *et al.* 2013), deposited by cohesive debris flows, equivalent of ungraded Ta division of Bouma (1962).

Facies 2. – Description: Thirty-two beds located in most sections (except sections 5, 10 and 11), from 0.3 m to 5.7 m thick (mean thickness 2.05 m). Almost the entire thickness or greater part of the bed consists of massive, structureless, ungraded grain-supported fine to medium-grained (in one bed coarse-grained) sandstone with 6–15% of mud matrix. In the upper part of the beds, the sandstone passes abruptly into a thin (1–50 cm) layer of dark, slightly graded mud with very fine sand admixture, commonly with coalified, dispersed plant detritus (Figs 9, 10A, 11B, 14E). Mudstone clasts, some of them well-rounded, rarely contorted, occur concentrated in the middle or upper parts of six beds, the thickness of which varies from 0.6 m to 5.0 m. Two beds contain dispersed, very coarse quartz grain or small quartz pebbles.

Interpretation: The sandstone part of Facies 2 corresponds to the interval TA of Talling *et al*. (2012) (subfacies Cs6 of Talling *et al*. 2013), graded mudstone in the uppermost part of the bed corresponds to the interval TE-2 in the Bouma sequence modified by Talling *et al*. (2012), or Te division *sensu* Bouma (1962). This facies records deposition from cohesive debris flow of the first phase of the flow event that changed into mud-density flow, *i.e.* turbidity current, towards the end of the flow event.

Facies 3. – Description: Two beds, 3.20 m and more than 4.0 m thick, in sections 3 a 6. In the section 3, the major part of the bed consists of clast-supported, massive, ungraded fine- to medium-grained sandstone, with 8–14% of clay matrix with floating very coarse quartz grains and small quartz pebbles up to 8 mm in diameter. In the section 6, mud clasts, some of them well rounded, occur in the middle and upper parts of the bed (Fig. 11A). An interval of deformed, convolute (wavy) lamination overlain by a thin layer of graded mudstone forms the upper part of these beds. The deformation of laminae does not affect the upper boundaries of the beds. In the section 3, the convolute lamination is highlighted by coalified plant detritus and clay, while in the section 6 it is manifested by deformation within the fine-grained sandstone (Fig. 11C, D).

Interpretation: Massive, ungraded sandstone part of the beds corresponds to the interval TA of Talling *et al.* (2012) (subfacies Cs6 of Talling *et al*. 2013) or ungraded Ta Bouma's division; convolute lamination corresponds to the interval TC *sensu* Talling *et al*. (2012) or Tc division of Bouma. The layer with convolute lamination is interpreted as horizontal lamination deformed during or immediately after deposition of the layer, probably due to the escape of water from rapidly deposited sand. In this sense the described lamination could be the deformed division Td in the Bouma's sequence. The beds were deposited from cohesive debris flow that passed towards the end of the flow event into low-density turbidity current (convolute laminated interval) resp. mud-density flow, *i.e.* turbidity current (graded mudstone, interval TE-2 in the Bouma sequence adapted by Talling *et al*. 2012, Te Bouma's division).

Facies 4. – Description: This facies includes four beds from sections 1, 6 and 10, ranging in thickness from 0.15 m to 2.5 m. It is distinct by the occurrence of horizontal lamination, which is formed by accumulations of coalified plant detritus with clay admixture. Three subfacies can be distinguished in this facies. Subfacies F4a is represented by one bed, 0.40 m thick, from section 1, where it exhibits three textural intervals: massive, ungraded fine- to medium-grained sandstone with 8% clay mud at the bottom, laminated sandstone in the middle, and graded mud at the top. Subfacies F4b consists of two beds, 0.12 m and 2.5 m thick, from sections 10 and 6, respectively. In these, a laminated interval at the top of the beds overlies ungraded clast-supported fine- to medium-grained sandstone with 8–10% clay matrix. The bed from section 6, 2.5 m in thickness, contains abundant mud clasts in two levels (Figs 7, 10B). Subfacies F4c is represented by a single, 0.12 m thick, laminated bed of clast-supported fine- to medium-grained sandstone with

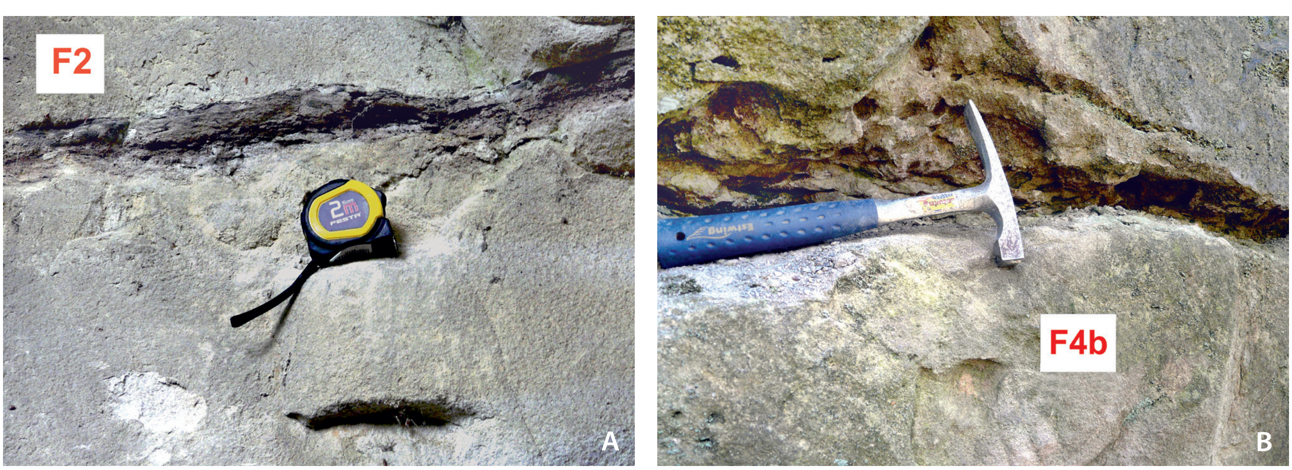

Figure 10. Sedimentary features in the Merboltice Fm. • A – upper part of the bed with a thin mudstone layer in the top. The erosive base of the overlying beds (Facies 2) illustrates partial erosion of the mudstone layer, section 9, abandoned quarry near the Ryjice village. • B – mud clasts concentrated into wavy layer in the ungraded division of the bed of Facies 4b, section 6, abandoned quarry in the Zubrnice village.

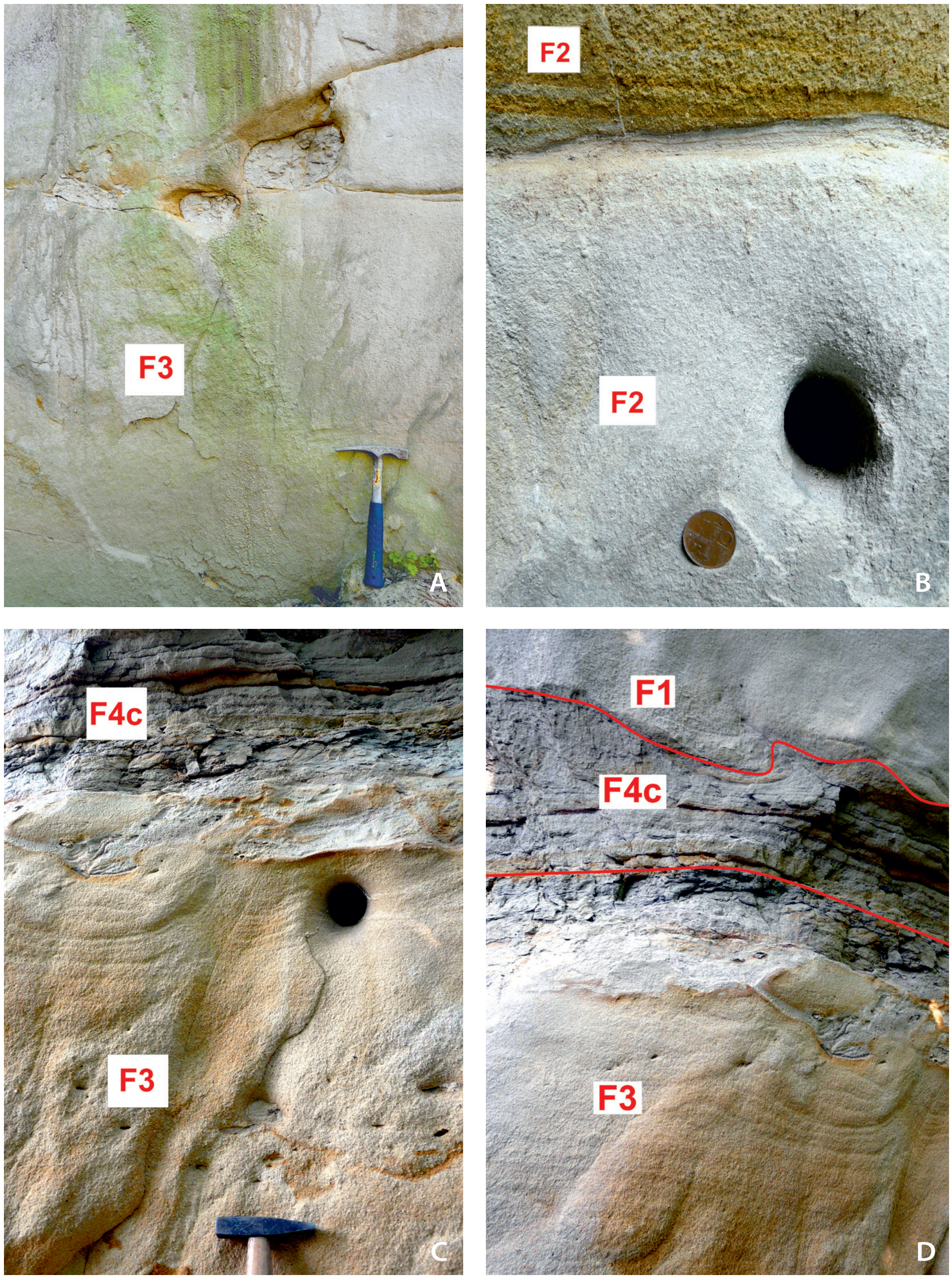

Figure 11. Sedimentary features in the Merboltice Fm. • A – well rounded mud clasts in the ungraded division of the bed Facies 3, section 6, abandoned quarry in the Zubrnice village. • B – detail of upper part of bed with very thin mudstone layer in the uppermost bed part (Facies 2), section 2, abandoned quarry near the Mírkov village. Artificially carved hole in the sandstone was used for wooden pin. Diameter of the coin is 2.4 cm. • C – convolute (wawy) lamination in the upper part of the bed Facies 3, section 6, abandoned quarry in the Zubrnice village. Artificially carved hole in the sandstone was used for wooden pin. • D – detail from the identical part of the section as in Fig. 11C. The bed of Facies 3 with convolute (wawy) lamination is superimposed by horizontally laminated bed of Facies 4c, the upper part of which was deformed after the deposition of the bed of Facies 1. Very irregular base of the bed of Facies 1 indicates the occurrence of imprints. Artificially carved hole in the sandstone was used for wooden pin.

8–10% clay matrix in section 6. In the upper part of the bed, the lamination is deformed by an irregular pressure of the overlying sediment and follows the uneven base of the overlying bed (Fig. 11D).

Interpretation: Intervals TA, TB, TD, and TE-2 of the Bouma sequence adapted by Talling *et al*. (2012) corresponding to the Ta, Tb, Td, and Te intervals of Bouma's sequence are represented in the Facies 4. The massive, ungraded sandstones at the base of the beds of subfacies F4a and subfacies F4b are interpreted as deposits of high-density turbidity currents due to their low thickness and the absence of floating coarse grains

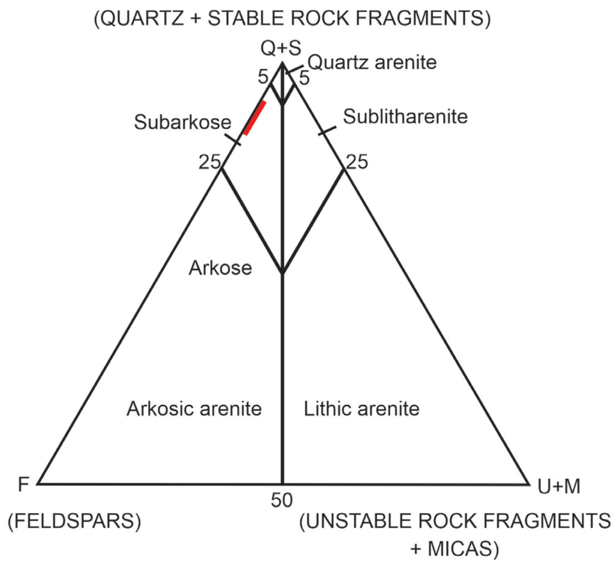

Figure 12. Sandstones of the Merboltice Fm. (narrow red box) in Dott's (1964) classification diagram modified by Pettijohn *et al.* (1972).

and pebbles (*cf.* Shanmugan 1997). The laminated interval present in all subfacies was deposited by high-density or low-density turbidity currents. Graded mud in the top of the subfacies F4a was deposited by mud-density flow, *i.e.* turbidity current. The two beds of subfacies F4b contain intervals TA and TB of Talling *et al.* (2012) and Ta and Tb Bouma's divisions, respectively. The subfacies F4c corresponds to the TB or TD interval of Talling *et al.* (2012) and to Tb or Td Bouma's divisions.

Facies 5. – Description: three beds from sections 4, 7 and 11 ranging in thickness from 1.6 to more than 4.0 m. These beds are characterized by normal gradation, ranging from medium- to coarse-grained sandstone to fine-grained and silty-clayey sandstone to graded mudstone, and in the case of section 11 to very fine-grained, light-coloured, silty-clayey sandstone (Figs 6C, 8). The sandstones are clast-supported and contain 8–12% of clay matrix.

Interpretation: Beds from section 4 and 7 exhibit the intervals TA and TE-2 as defined by Tallings *et al.* (2012, 2013) or the Ta and Te divisions in the Bouma's sequence. The bed from section 11 corresponds to interval TA or division Ta. Normal gradation in this facies indicates deposition from a high-density (sandy) turbidity current followed, in the beds from sections 4 and 7, by mud density flow (Talling *et al.* 2012).

Facies 6. – Description: In sections 4 and 10, thin layers of faint greenish, light grey ungraded mudstone, 3–4 cm thick, were found. In section 4 (at the 8.0 m level) the mudstone layer sharply overlies the dark grey graded

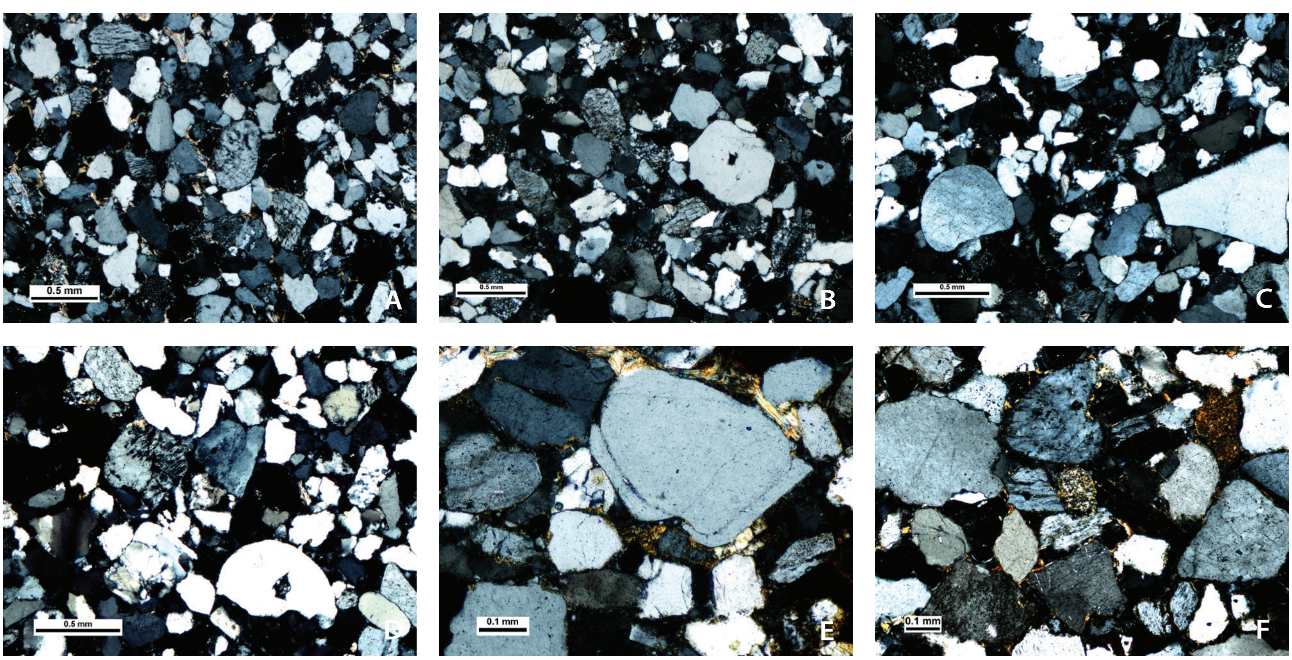

Figure 13. Petrology of the Merboltice Fm. sandstones. • A – section 11, Hibsch cave, 0.55 m, moderately sorted subarcose, rounded K-feldspar grain in the middle of the picture, feldspar grains above the scale are sericitized. Crossed polars. • B – section 2, Mírkov, −0.50 m, less to moderately sorted subarcose, feldspar grains are nearly unaltered or only slightly altered. Crossed polars. • C – section 2 Mírkov, −0.50 m, poorly sorted (bimodal) subarcose, floating quartz grains in the coarse fraction exhibit contrasting roundness. Crossed polars. • D – section 10, Krásné Březno, −0.65 m, moderately sorted subarcose, right of scale floating broken well rounded quartz grain (textural inversion). Crossed polars. • E – section 2 Mírkov, 7.20 m, poorly sorted subarcose, in the middle of the picture rounded quartz grain with partly abraded rim of SiO_2. Crossed polars. • F – section 4, Březiny, 5.50 m, less sorted subarcose, cluster of feldspars in different alteration stages, from unaltered to strongly sericitized. Crossed polars.

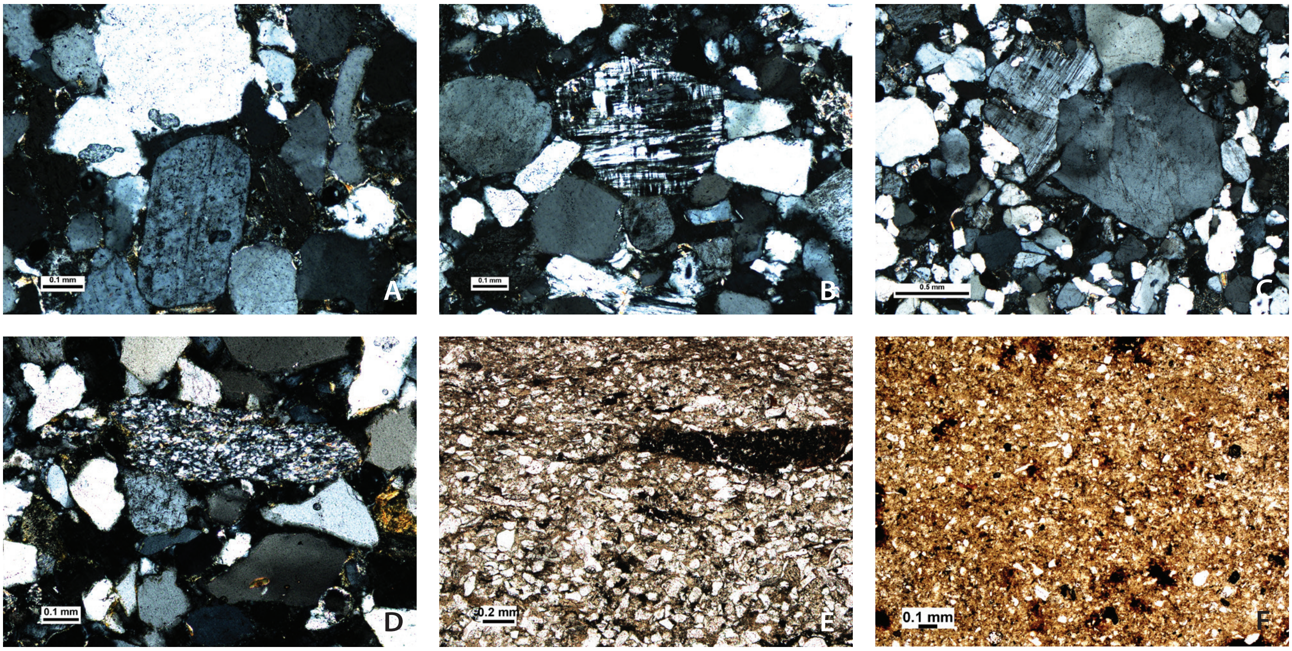

Figure 14. Petrology of the Merboltice Fm. sandstones and mudstones. • A – section 10, Krásné Březno, −0.35 m, less sorted subarcose, in the lower part of the photo a cross-section of columnar, nearly unrounded, unaltered K-feldspar. Crossed polars. • B – section 2, Mírkov, −2.30 m, nearly unaltered grain of microcline (in the middle of the photo, the upper edge of the grain is weakly sericitized) in the less sorted subarcose. Crossed polars. • C – section 2, Mírkov, −0.50 m, less to moderate sorted subarcose with floating coarse granitoid clast consisting of quartz and unaltered plagioclase grains. Crossed polars. • D – section 4, Březiny, 3.00 m, less to moderately sorted subarcose, elongated grain of very fine-grained micaceous quartzite in the upper part of the picture. Crossed polars. • E – section 9, Ryjice, −0.05 m. Transition of subarcose to mudstone (upper part of thin section) near the top of the basal bed. Small scattered dark fragments of coalified plant matter and large fragment of coalified wood are visibles. • F – section 4, Březiny, 8.02 m, mudstone of the Facies 6 forming a thin layer between two beds deposited from gravity flows.

mudstones that form the top of the underlying Facies 2 (Fig. 7). In section 10 (at the −0.15 m level) the mudstone layer sits sharply on a bed of ungraded sandstone (Fig. 8). The terrigenous quartz grain content in the silt, and, to a smaller extent, also in the very fine sandy fraction, is about 20%. There are no fragments of coalified plant detritus (Fig. 14F).

Interpretation: These mudstones represent *in situ* sediment that was deposited from suspension in the pause between gravity flows. The ungraded mudstones from sections 4 and 10 are comparable to interval TE-3 of Talling *et al*. (2012).

Petrography

The petrographic composition of the Merboltice sandstones was analysed in forty-four samples from nine localities. Sandstones with a grain-supported structure are mostly composed of three main components: quartz, feldspars and clay matrix (Tab. 1). With a few exceptions the matrix content does not exceed 15%, therefore, the modified diagram of Dott (1964) was used for classification of the sandstones (Fig. 12). The diagram shows very little variation in the composition of the sandstones, which fall within a narrow range of subarcoses. The other components are present in accessory amounts, generally ranging from < 1 to 2–3% (Tab. 1).

Quartz contributes on average 78.5% to the composition of the sandstones with extreme values of 70% and 85% respectively. Monocrystalline grains predominate over polycrystalline grains, forming *ca*. 85–90% of the quartz. Roundness was evaluated visually and the grains were divided into five classes according to Krumbein (1941). Subangular grains represent the majority of grains (*ca*. 65–70%) and sub-rounded grains form a maximum of 15–20%. Angular grains (*ca*. 10–15%) are also present. Well-rounded grains are very rare (< 1%). Contrasting roundness can often be observed in grains of the same grain size (Fig. 13C). There are also rounded grains with a sharp-edged broken part or broken rounded grains (textural inversion, Fig. 13D). Rarely, grains with a partially abraded syntaxial rim occur (Fig. 13E). The mean grain size varies in a narrow span between 0.20–0.37 mm. Sorting (Fig. 13A–F) was observed visually. Poor to moderate sorting predominates, less frequently the sorting is well, very rarely very well. The poor sorting is influenced by the presence of scattered coarse grains in the predominant fine- to medium-grained fraction and also by the admixture of grains below 0.063 mm (silt). With a greater

Table 1. Distribution of major components in thin sections of sandstones and mudstones of the Merboltice Fm.

Locality, metrage	Qtz	Kfs	Plg	Sorting	S.R.	U.R.	Mean gs.	Max. gs.	Roundness	Ms	C.P.D.	C.M.	B.I.	Grains & Notes
Mírkov −2.30 m	80	10	1	2	1–2	0	0,30	1,5	a < sa > sr >> r	< 1	0	6–7	0	1 Mc
Mírkov −0.50 m	80–82	8–10	1	2, bmd	1	<<< 1	0.30–0.32	1,7	a < sa > sr >> r	0	0	8–10	0	2 grnt
Mírkov 0.40 m	82–83	8	1	2–3	< 1	0	0.25–0.27	1,3	a < sa > sr >> r	< 1	1	7–8	0	
Mírkov 0.88 m	79–80	8	< 1	3–4	0	0	0.20–0.23	0,6	a < sa > sr >> r	< 1	< 1–1	12	0	
Mírkov 0.95 m	75–77	8	< 1	2–3	< 1	0	0.20 – 0.25	0,9	a < sa > sr >> r	< 1		15	0	
Mírkov 6.70 m	75–77	8–10	1	3–4	< 1	0	0.25–0.27	0,8	a < sa > sr >> r	< 1		12	0	1 Mc
Mírkov 7.20 m	79–80	10	1	2	< 1	0	0. 25–0.30	0,9	a < sa > sr>> r	< 1		10–12	0	1 myr
Mírkov 8.00 m	82–84	8	< 1	2–3	< 1	0	0.25–0.27	1,2	a < sa > sr >> r	< 1		8	1	1 *
Mírkov 8.50	80–82	8–10	1	3	1	0	0.23–0.25	1,3	a < sa > sr >> r	< 1		7–8	0	1 Mc
K. Březno −0.65 m	82–84	6–7	< 1	3	3	0	0.25–0.27	0,9	a < sa > sr	< 1	< 1	6–8	0	2 Mc
K. Březno −0.45 m	70–72	6–8	< 1	2	< 1	0	0.23–0.25	0,7	a < sa > sr >> r	< 1	4–5	15	0	3 Mc
K. Březno −0.35 m	75–77	8	< 1	2, bmd	2	0	0.28–0.30	1,1	a < sa> sr >> r	<< 1	0	13–15	0	1 Mc
K. Březno 0.10 m	78–80	8	< 1	4	< 1–1	0	0.23–0.25	0,8	a < sa > sr >> r	< 1	3	8–10	0	1 Mc
K. Březno 1.30 m	76–78	10	< 1	4	< 1	<<< 1	0.21–0.23	0,4	a < sa > sr >> r	< 1	2	10	1	1 grnt, Mc, Glt
Březiny 0.50 m	80–84	6–8	< 1	1–2, bmd	4	<<< 1	0.40–0.50	1,8	a < sa > sr >> r	< 1	0	6–7	0	1 grnt
Březiny 2.00 m	80–82	6–7	< 1	3	1	<<< 1	0.28–0.30	1,3	a < sa > sr >> r	<< 1	< 1	10	0	1 Mc & grnt
Březiny 3.00 m	80–82	9–10	< 1	2	< 1–1	<<< 1	0.24–0.26	1,0	a < sa > sr >> r	<< 1	0	7–8	0	1 grnt; 1 Bt
Březiny 3.90 m	85–87	5	< 1	3–4	< 1	0	0.22–0.23	0,9	a < sa > sr >> r	< 1	< 1	6–7	0	1 myr
Březiny 4.50 m	83–85	7–8	< 1	2–3	2	0	0.35–0.37	0,9	a < sa > sr >> r	<< 1	0	6–7	0	1 Mc & myr
Březiny 5.50 m	76–78	8–10	1	2	2–3	0	0.26–0.28	0,9	a < sa > sr	<< 1	0	10–12	0	2 Mc, myr; 1 Bt
Březiny 6.50 m	77–79	10–12	< 1	3	3	0	0.26–0.28	1,3	a < sa> sr	0	0	7–8	0	
Březiny 7.50 m	77–79	8–10	< 1	3	1	0	0.24–0.26	1,0	a < sa > sr >> r	< 1	0	10	0	1 Mc, myr
Březiny 8.02 m	28–30	< 1			<< 1	0	0.04–0.045	0,0	a < sa>>sr	< 1–1	< 1–1	75–77	0	mdst
Merboltice 1.30 m	73–75	12–13	1	2–3	1	0	0.20–0.22	1,9	a < sa > sr >> r	< 1	1	10–12	0	
Merboltice 2.95 m	77–78	8	< 1	2	< 1	0	0.28–0.30	1,6	a < sa> sr >> r	0	1	12–13	0	
Merboltice 3.50 m	79–80	10	1	2–3	1	0	0.18–20	0,8	a < sa > sr >> r	1–2	0	8–10	0	
Merboltice 5.90 m	75–77	12–13	1	2–3	1	0	0.20–0.22	0,8	a < sa > sr >> r	1–2	1	10	0	1 Mc
Merboltice 6.35 m	82–84	6–8	< 1	2–3	1	0	0.20–0.22	0,7	a < sa = sr >> r	< 1	0	10	0	
Merboltice 8.35 m	70–72	13–15	1–2	1–2	1–2	0	0.20–0.22	1,3	a < sa > sr >> r	< 1	0	10	0	
Ryjice −2.10 m	73–75	10	1–2	2	< 1	0	0.24–0.26	4,0	a < sa > sr >> r	<< 1	< 1	13–15	0	1 Mc
Ryjice −1. 00 m	79–80	6–8	1	2–3	< 1	0	0.28–0.30	0,9	a < sa > sr >> r	< 1	< 1	12	0	
Ryjice −0. 35 m	78–82	6–8	< 1	2	< 1	0	0.28–0.30	0,8	a < sa > sr >> r	<< 1	0	12–14	0	1 Mc
Ryjice −0. 05 m	25–35	3–4	<< 1	3	<< 1	0	0.15–0.04	0,2	a < sa > sr	3–4	4–5	40–60	0	mdst
Ryjice 0. 25 m	76–78	7–9	1	2	1	0	0.28–0.30	0,9	a < sa > sr >> r	<< 1	<< 1	10–12	0	3 Mc
Ryjice 1. 10 m	78–80	8–10	1	2–3	1–2	0	0.28–0.30	1,3	a < sa > sr	< 1	<< 1	8–9	0	1 Mc
Hibsch cave −2.60 m	77–80	8–10	< 1–1	2–3	< 1–1	0	0.28–0.30	1,0	a < sa > sr	< 1	0	8–10	0	2 Mc
Hibsch cave −0.35 m	88–90	5–6	< 1	4	< 1	0	0.21–0.23	0,5	a < sa > sr >> r	< 1–1	0	5–6	0	1 Mc
Hibsch cave −0.10 m	36–40	2	<< 1	2	< 1	0	0.21–0.23	0,5	a < sa > sr	< 1	0	58–62	0	
Hibsch cave 0.55 m	76–78	7–8	< 1	2–3	2	0	0.28–0.30	1,3	a < sa > sr >> r	< 1	0	12–13	0	
Hibsch cave 4.00 m	82–84	6–7	< 1	2–3	< 1	0	0.28–0.30	1,3	a < sa > sr	<< 1	0	10–12	0	1 Mc
Maškovice 2.50 m	82–84	5–6	< 1	3–4	<< 1	0	0.23–0.25	0,6	a < sa > sr	< 1–1	0	10–12	0	
Maškovice 5.80 m	83–85	5–6	< 1	2	< 1–1	0	0.35–0.37	1,7	a < sa > sr	< 1	0	10–12	0	myr
Myštice 11.00 m	82–85	6–8	1	1–2, bmd	< 1	<<< 1	0.45–0.55	2,8	a < sa > sr >> r	<< 1	0	8–9	0	1 grnt, Mc; 2 myr
Zubrnice −2.50m	78–80	10–12	1	3	1	<<< 1	0.28–0.30	1,8	a < sa > sr >> r	<< 1	<< 1	10	0	1 grnt, 2 Mc

Abbreviations: B.I. – bioturbation index; bmd – bimodal; Bt – biotite; C.P.D. – coalified plant detritus; C.M. – clayey matrix; Glt – glauconite; grnt – granitoid; gs. – grainsize; Kfs – K-feldspar; Max. gs. – maximum grainsize; Mc – microcline; mdst – mudstone; Ms – muscovite; myr – myrmekite; Plg – plagioclase; Qtz – quartz; S.R. – stable rocks; U.R. – unstable rocks. Legend: Sorting: 1 – very low, 2 – low, 3 – medium, 4 – good. Roundness: a – angular, sa – subangular, sr – subrounded, r – rounded. Notes: * – bioturbation tunnel of mm diameter.

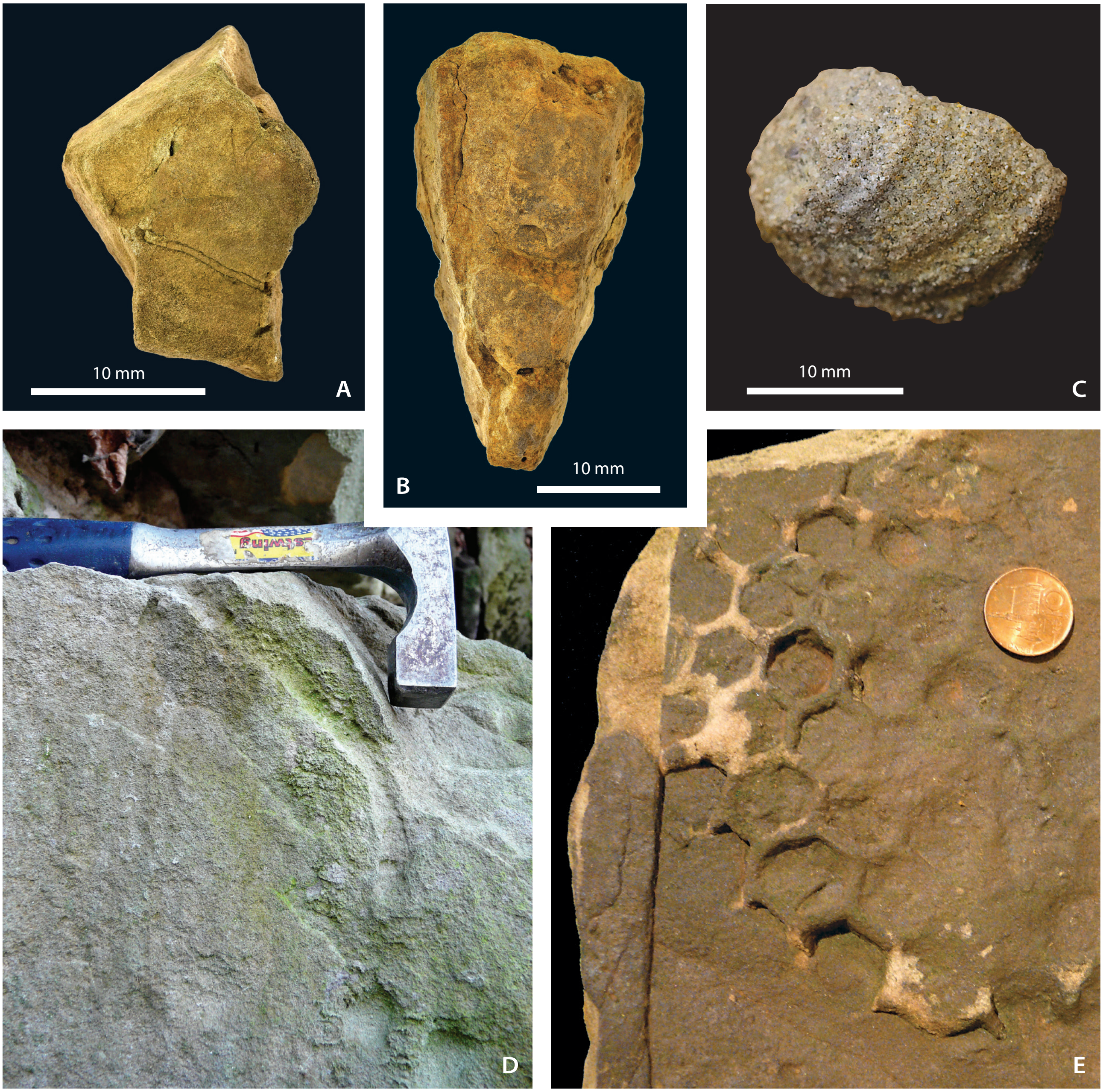

Figure 15. Trace fossils and fossils in Merboltice Fm. • A – ichnogenus *Planolites*?, locality Těchlovice near locality 1 (borehole SK-12c Těchlovice). Collections of Municipal Museum of Ústí nad Labem. Inventory No. G 29987. Photo by J. Preclík. • B – branching tunnel of the ichnogenus *Ophiomorpha*, locality Těchlovice near locality 1 (borehole SK-12c Těchlovice). Collections of Municipal Museum of Ústí nad Labem. Inventory No. G 29986. Photo by J. Preclík. • C – *Inoceramus* sp. from section 3, abandoned quarry in the Merboltice village. Collection of S. Čech. Photo by S. Čech. • D – *Ophiomorpha* ichnogenus tunnel on section 10, abandoned quarry in the Krásné Březno village. • E – ichnogenus *Paleodyction*, locality Těchlovice near locality 1 borehole SK-12c Těchlovice. Collections of Municipal Museum of Ústí nad Labem. Inventory No. G 29984. Diameter of the coin is 2.4 cm. Photo by J. Preclík.

admixture of floating coarse grains, the sandstones are bimodal (Fig. 13C). Similar conclusions were also reached by Zelenka (1980), who found that, in the sense of Folk (1954), the sandstones were "slightly sorted".

Feldspars contribute on average 8% to the composition of the sandstones, with extremes of 6% and 15%. The ratio of K-feldspars to identifiable plagioclase is *ca*. 10:1 to 8:1. The plagioclase probably includes most of the completely kaolinized or sericitized grains (Fig. 13A, F). Identifiable K-feldspar grains are grey to blue-grey in colour and are nearly unaltered or slightly altered (Figs 13A, B; 14A, B). Feldspar grains are mostly subangular, less frequently suboval. Oval grains were also found in two thin sections (Fig. 13A). The K-feldspars partly retain a prismatic shape,

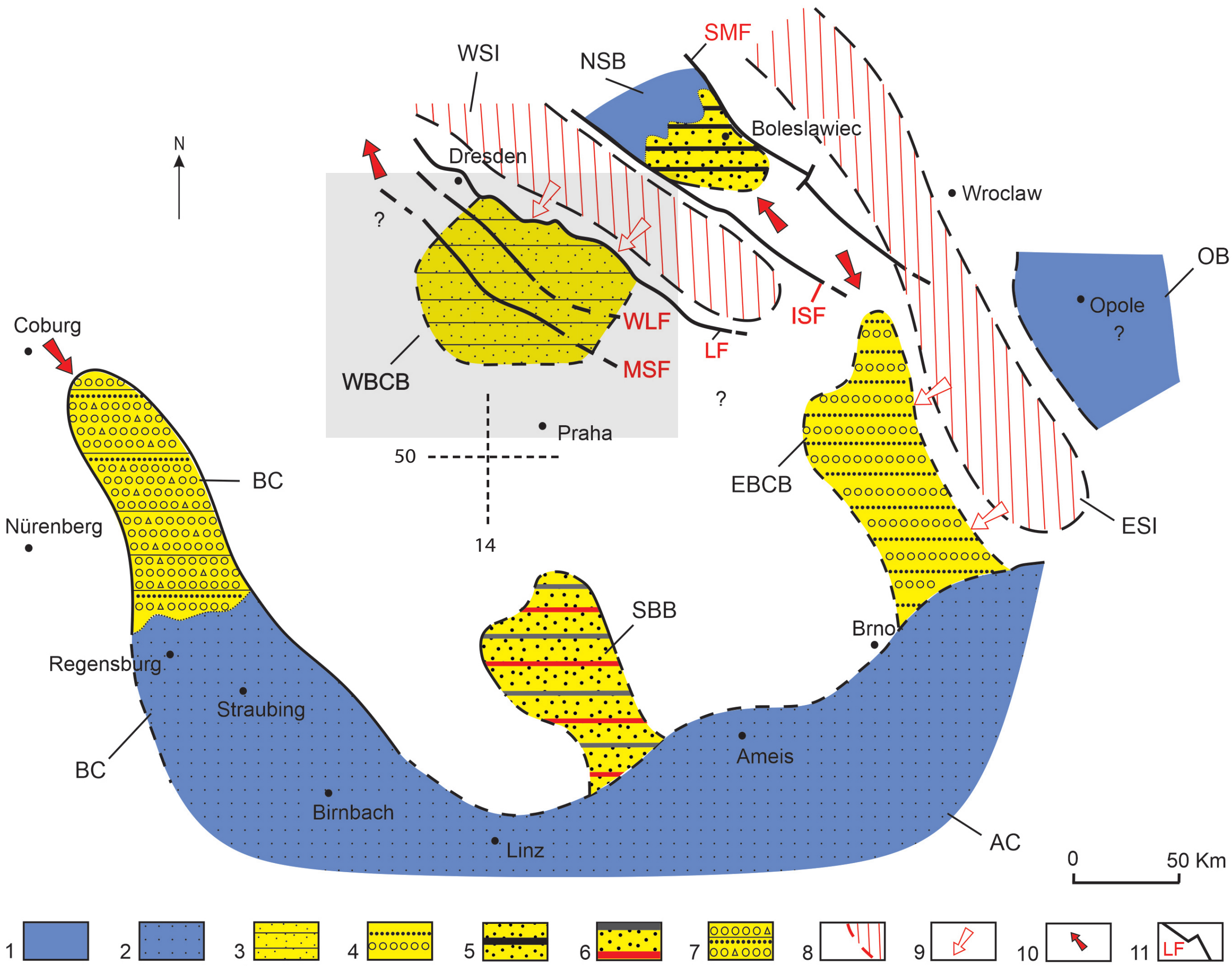

Figure 16. Palaeogeographical situation in the Santonian in the Bohemian Massif and adjacent areas. (Area of the North Sudetic Basin around Boleslavec modified after Milewicz 1997). Abbreviations: AC – autochthonous Cretaceous on the southern and south-eastern slopes of the Bohemian Massif; BC – Bavarian Cretaceous (Regensburg Basin or Regensburg Gulf); EBCB – eastern part of the Bohemian Cretaceous Basin; NSB – North-Sudetic Basin; OB – Opole Basin; SBB – South Bohemian Basin; WBCB – western part of the Bohemian Cretaceous Basin. Legend: 1 – calcareous mudstones, marlstones; 2 – marlstones, sandy mudstones and calcareous fine- to medium-grained sandstones; 3 – fine- to medium-grained sandstones of the Merboltice Fm.; 4 – sandstones and conglomerates; 5 – sandstones with claystones and coal seams (deltaic sedimentation); 6 – cyclic sedimentation of conglomerates, sandstones and dark and varicoloured claystones; 7 – conglomerates and breccias with claystone intercalations; 8 – major source areas during the sedimentation of the Březno Fm. (Coniacian) in the north-eastern marginal part of the Bohemian Massif (WSI – West Sudetic Island, ESI – East Sudetic Island); 9 – main directions of detrital input to the western and eastern part of the Bohemian Cretaceous Basin in the Santonian; 10 – regression directions; 11 – important faults (LF – Lusatian Fault, ISF – Intra Sudetic Fault, SMF – Sudetic Marginal Fault, WLF – West Lusatian Fault, MSF – Mid-Saxonian Fault).

sometimes only slightly affected by transport (Fig. 14A). One to three grains of microcline were found in twenty thin sections (Fig. 14B). Five thin sections contain one to two grains with letter-like intergrowth of quartz and feldspar (myrmekite). The fragments of stable rocks are represented by quartzites and very fine-grained silicites, occurring in all thin sections in amounts up to 2–3%, rarely 4%. The quartzites include polycrystalline grains with a large number of equal-sized grains, elongated grains, or elongated sutural grains. A few grains are fine-grained sericitic quartzites (Fig. 14D). Fragments of unstable rocks were found in seven thin sections. They were always granitoid clasts, consisting of a few quartz and feldspar phenocrysts. The clasts are found in the coarse fraction, ranging in size from 0.8 mm to 1.8 mm. The largest granitoid clast consisting of quartz phenocrysts and only slightly altered plagioclase was found in the section 2 (Fig. 14C). The micas are represented by muscovite (Fig. 14A), which occurs in quantities of up to 1–2%. In two thin sections, one biotite flake with typical pleochroism was found. Glauconite was found in a single thin section as an isolated dark green oval grain, 0.15 mm in size. Small fragments of coalified plant detritus and rarely centimetre-sized fragments of leaves and wood, occur locally in the sandstones. The clay matrix has both coating and porous character. Its content varies from 6 to 15%. According to the analytical data of Gabriel (1984), the matrix content ranges from 6.4% to 17.6% and is composed of kaolinite. Mudstones at the top of the beds deposited from gravity flows are dark grey. The contents of terrigenous quartz in the silt, and subordinately in the fine sandy fraction floating in the clay matrix, is around 20–25%. Feldspar grains in mudstones are less frequent compared to sandstones, the content is only around 3–4%. Fragments of coalified plant detritus are common in mudstones, and fragments of leaves or wood up to 5–6 cm in size also occur (Fig. 14E).

Trace fossils

Trace fossils are rarely found in the Merboltice Fm. and occur within the sandstones (endichnia) and on their lower bedding planes (hypichnia). The trace fossils described below come from the author's findings and from the findings of T. Durdinec, deposited in the Municipal Museum of Ústí nad Labem. The findings of T. Durdinec (Fig. 15A, B, E) found close to the section 1 were published by Mikuláš & Vařilová (2021). Three types were identified in the endichnia group, which are shafts penetrating perpendicularly or steeply to the stratification:

1) A tunnel with smooth walls, 0.8–1.5 cm in diameter, penetrating subvertically to a depth of at least 2 m, filled with material identical to the surrounding sandstone; morphologically, it is similar to the ichnofossil *Planolites* (Fig. 15A), but it cannot be classified with certainty.

2) Tunnels penetrating into the depth of 0.5 m below the upper surface of a 1.9 m thick bed in the section 3 (Fig. 7); these tunnels have a diameter of 1–1.5 cm and are filled with mud from the top of the bed; they are probably dwelling structures representing colonization of the bottom during a pause between successive gravity flows.

3) Tunnels with a diameter of about 1.5–2 cm penetrating perpendicularly to obliquely to the bedding surface to a depth of *ca*. 0.4 m in the section 10; small negatives of the bumps covering the surface of the tunnels are visible on the inner surface of the tunnels (Fig. 15B, D); morphologically, this type corresponds to the ichnogenus *Ophiomorpha*; a typical ichnogenus *Ophiomorpha* from the T. Durdinec findings was also described and illustrated by Mikuláš & Vařilová (2021).

Among the hypichynia, a regular network structure with positive relief, typical of the ichnogenus *Paleodyction*, was found on the lower bedding surface (Fig. 15E). A similar ichnofossil, found in the Elbe Valley in the outcrop near section 1, was published as *Paleodyction* by Prinz (1930). According to archetypal depth zonation by ichnofossils, the ichnogenus *Ophiomorpha* was considered as an indicator of shallow-water, marine environment, while the ichnogenus *Paleodyction* was usually considered an indicator of a deep-water environment. However, these ichnogenera have been found in both shallow and deep-water environments (*e.g*. Seilacher 2007, Fürsich *et al.* 2007, Demircan & Uchman 2017). Hence, scarce trace fossils cannot be used to determine the depth at which the Merboltice Fm. was deposited.

Discussion

Depositional processes – flow dynamics

Textural and structural analysis presented in section 5 suggests that most of the beds in the Merboltice Fm. were deposited during a flow event which began as a cohesive flow changing during the flow vanning into turbidity current. The beds are composed of debrites transitioning at their tops into turbidites (Facies 2 and 3) due to an event that comprises two different types of flow. The succession of different flow types during individual flow events is evidenced by Mulder & Alexander (2001), Amy *et al*. (2005) or Talling *et al*. (2012, 2013). According to Amy *et al.* (2005) these are "cogenetic turbidite-debrite beds", according to Talling *et al.* (2012) "linked turbidite-debrite beds". Only a small number of the beds was deposited either from cohesive flows as debrites (Facies 1) or from turbidity current as turbidites (Facies 4 and 5). Debrites deposited during en masse consolidation of sand without size segregation (abrupt freezing of sandy detritus). A content of clay matrix in the order of the first percentages is sufficient to form a debris flow (Hampton 1975, Shanmmugan 1997, Marr *et al*. 2001, *etc*.). The predominance of debrites in the Merboltice Fm. was made possible by the content of clay matrix, not dropping below 6–7%, usually around 10%, often even more, between 12% and 15%. Gabriel (1984) mentioned clay matrix content up to 17.6% from the present-day abandoned sand pit Zálezly near Ústí nad Labem. Talling *et al*. (2012) defined 12% mud content in massive sandstones at the boundary between cohesive flows (above 12% mud) and poorly cohesive flows (below 12% mud). According to their concept, the massive, ungraded sandstones of the Merboltice Fm. represent a continuous transition from poorly cohesive to cohesive gravity flows.

Provenance

The character of source rocks can be determined by heavy minerals (HM) associations (Tab. 2), feldspar content,

Table 2. Distribution of heavy minerals in the subarcoses of the Merboltice Fm. (mean values from 17 analyses taken at outcrops and in boreholes).

	Rutile	Zircon	Tourmaline	Monazite	Garnet	Staurolite	Anatase	Kyanite	Titanite	Topaz
Number of grains	205	583	232	27	8	6	36	1	6	1
Percentage	18.5	52.9	21.08	2.4	0.7	0.54	3.2	0.09	0.5	0.09

the nature of rock fragments and grain roundness. The HM association is strongly dominated by ultrastable minerals (Tab. 2). Due to the relatively low mineralogical maturity of the Merboltice sandstones, the ZTR index (zircon, tourmaline and rutile content; Hubert 1962) is striking high, reaching 92.48% a value reported for quartz sandstones (orthoquartzites). The ZTR index indicates a significant proportion of older, mainly Cretaceous, sediments in the source, which was already assumed by Slavík (1988). A large contribution of recycled sediments to the composition of sandstones was also found in the nearby North Sudetic Basin (Biernacka 2012). The negligible content of other HM can be explained by 1) their long diagenetic dissolution in older Cretaceous, mainly psammitic sediments, before their erosion and redeposition (Morton & Hallsworth 1999, Garzanti 2017); and 2) the warm and mostly humid climate (see below), which led to their dissolution in the weathering mantle (Garzanti & Ando 2007). At the Merboltice type locality (section 3 in Fig. 7), Nádaskay *et al*. (2019) found an abrupt change in the proportion of Variscan-age zircons from 23% in the underlying Březno Fm to 48.5% in the Merboltice Fm. This change can be explained in terms of an increased contribution from the Variscan Krkonoše-Jizera Plutonic Complex in the south-eastern part of the source area. Relatively high feldspar content, with little alteration of K-feldspars, which often preserve prismatic shapes, together with granitoid clasts, demonstrate a significant contribution from granitoids. The very low plagioclase content was probably influenced by the warm and humid climate (see below). Chemical weathering reduced the feldspar content, preferentially of the less stable plagioclase in the weathering section (Johnsson 1993, Garzanti 2017). According to James *et al*. (1981), a humid climate reduces the plagioclase content of fluvial sediments to one third. The small proportion of plagioclase may also be related to the significant presence of K-feldspar-dominated monzogranites in the adjacent source. In the source area (West Sudetic Island, Fig. 16), the Lusatian granitoid Massif was exposed over a considerable area during the Cretaceous sedimentation (Skoček & Valečka 1983). One of the main granite types is the Rumburk monzogranite to granodiorite (Kozdrój *et al*. 2001), in which K-feldspars prevail over the plagioclase (Opletal *et al*. 2006). This monzogranite is exposed at the present-day erosional level over a large area adjacent to the Lusatian Fault. It is likely that the monzogranite provided detritus already during the deposition of the Merboltice Fm. Grains of quartzites, partly micaceous and silicites suggest an additional contribution from metamorphites. The metamorphites also yielded strongly elongated, partly lance-shaped quartz grains. Grain roundness is considered to be a poorly indicative factor (Garzanti 2017). Well-rounded grains, grains with partially abraded SiO_2 rims and broken rounded grains (structural inversion) can be considered as an evidence of redeposition of the parent, older Cretaceous (or also Permo-Carboniferous) rocks. Due to the modest extent and shape of the source area (Fig. 16), the river transport was short and did not allow a higher degree of rounding. The difference in rounding may also have been influenced by the duration of grain residence time in the nearshore (beach) zone. Some grains may have been rapidly transported from the coast to the basin, while others may have remained in the nearshore zone longer and reached a higher degree of roundness. A large difference in the roundness of the first-cycle material can be observed, among others, in the feldspars. In addition to the poorly rounded, prismatic grains, oval grains are also found.

Palaeogeography

Santonian deposits in the eastern part of the Bohemian Cretaceous Basin and in the other Cretaceous basins of the Bohemian Massif

The only other deposits of the Bohemian Cretaceous Basin that can be assigned to the Santonian are depositional relics in the Králíky Trench (Nysa Graben), south of Kladsko (Fig. 16). These deposits, are known as the upper part of the Idzikow Member resp. Idzikow sandstones and conglomerates and were interpreted by Jerzykiewicz (1970, 1971) as regressive, offshore sediments because they developed by coarsening from a predominantly pelitic flysch-like facies. Jerzykiewicz (1970, 1971) estimated their thickness at 200–320 m. Pebbles found in polymictic conglomerates in the upper part of the Idzikow Member suggest a source area in the vicinity of their occurrence, in the crystalline area of the Králický Sněžník Mts. Wojewoda (1997) also interpreted these deposits as nearshore, regressive sediments. They developed from the flysch-like facies described by Jerzykiewicz (1971) and Valečka (1984, 1988). The highest part of this facies in the Králíky Trench was classified as Lower Santonian by Hercogová (1985). The regressive sandstones and conglomerates are also classified as Santonian by Voigt *et al*. (2008) and Wojewoda *et al*. (2022), who estimated their thickness in contrast to Jerzykiewicz's data as little as 85 m.

Santonian strata outside of the Bohemian Cretaceous Basin include occurrences in the North Sudetic Basin. Santonian in this basin is characterized by a regressive development or in its south-eastern part, deltaic or coastal sandstones with clay and coal layers are deposited (prograded) over the marine sediments. Towards the NW, these deposits pass into marine calcareous mudstones (Milewicz 1997, Lezczyński *et al*. 2022). From the geographic position of the deltaic deposits in the North Sudetic Basin, it is clear that the connection of the North Sudetic Basin with the Bohemian Cretaceous Basin was interrupted and a watershed was created between the basins. Two source areas, the West Sudetic and East Sudetic Island still existing at the end of the Coniacian (Fig. 16), formed a connected complex. The detritus for Merboltice Fm. was primarily brought from the enlarged area of the former West Sudetic Island. Figure 16 shows the idea that the aforementioned watershed continued further to the SW and divided the Bohemian Cretaceous Basin (BCB) in two parts: the Merboltice Fm. formed in the western part of the basin (WBCB), while shallow-water Idzikow sandstones and conglomerates were deposited in the eastern part (EBCB).

The situation in the Opole Cretaceous Basin is unclear, marine marlstones to limestones are the youngest preserved sediments. Walasczyk (1992) and Kedzierski (2008) placed these sediments in the Middle Coniacian and considered the continuation of marine sedimentation into the Santonian as very likely. However, Santonian sedimentation is stratigraphically well documented at the southwestern, southern and south-eastern margins of the Bohemian Massif. On the opposite, a regression occurred in the Bavarian Cretaceous (Regensburg Basin or Regensburg Gulf) and terrestrial clastics, conglomerates, breccias and sandstones with claystone intercalations were deposited in its northern part in the Santonian (Tilmannn 1964, Meyer 1996). These fluvial and proluvial clastics, several-hundred-metres-thick, are defined by Niebuhr *et al.* (2009) as the Hessenreuth Formation. Upper part of these clastics (Hesserberg Member) at Auerbach is deposited on Coniacian marlstones and sandstones belonging to the Hellkofen and Jeding formations (Niebuhr *et al*. 2009). Further to the southeast, marine marlstones with beds of fine- to medium-grained sandstones were deposited in the Braunau Basin *sensu* Herm (1979) in the Santonian (Unger & Meyer 1996). These sediments covered by alpine molasse have been verified by drillings in Straubing and Birnbach (Tillmann 1964, Unger & Risch 1991). Further to the SE to E, on the southern and south-eastern slopes of the Bohemian Massif, marlstones, mudstones and calcareous sandstones were deposited, often with a high glauconite content, as evidenced by boreholes into the basement of the Alpine-Carpathian molasse and the Carpathian folds at Ameis, Poysdorf and on the southern Moravia (Řehánek 1978, Eliáš & Wessely 1990). These Santonian deposits, continuously following the Coniacian sedimentation are classified as Pálava Fm. of Lower Coniacian to Upper Campanian age (Bubík *et al*. 1995, Stráník *et al*. 1996) in the Pavlovské vrchy hills in southern Moravia. The palaeontological record in the Pálava Fm. demonstrates a broad connection with the Tethys area.

The South Bohemian Basin records continental sedimentation of a fluvial system that flowed into the marine area on the south-eastern slopes of the Bohemian Massif adjacent to the Tethys. In this basin, fluvial and lacustrine, cyclically arranged conglomerates, sandstones and claystones were deposited, sometimes coal-bearing, forming the Klikov Formation, several hundred metres in thickness. The upper part of this formation is classified as Santonian (Slánská 1974, Váchová 2007, Váchová & Kvaček 2009).

Control on gravity flows

The Merboltice Fm. deposited from gravity flows, represents an anomaly due to specific, local conditions in a sub-segment of the shrinking sedimentary basin within the Santonian sedimentation in the Bohemian Massif (Fig. 16). The analogous sedimentary sequence was not found in other basins in the Bohemian Massif. The formation follows the flysch-like facies of the Březno Formation, in which gravity (turbidity) flows were also active. The flysch-like facies was deposited only at the north-eastern margin of the Bohemian Cretaceous Basin, adjacent to tectonically active source areas that increased in extent during the Coniacian (Valečka & Rejchrt 1973; Valečka 1984, 1988; Valečka & Skoček 1991). However, the flysch-like facies is dominated by calcareous mudstones deposited in the shallow (shelf) environment of the open sea, as evidenced by the associations of bivalves, especially articulated *Nucula* and inoceramids (*e.g. Volviceramus* and *Platyceramus)* often in growth position and associations of shallow-water benthic foraminifera with abundant *Neoflabelina* and *Stensioenia* (Hercogová & Valečka 1977; Valečka 1984, 1988; based on data from S. Čech). The sedimentation of calcareous mudstones was occasionally interrupted by deposition of fine sandy turbidites, and tempestites, usually a few centimetres to decimetres thick. The ratio of the thicknesses of calcareous pelites to the sandy layers ranges from 15.9:1 to 56.9:1 (Valečka 1984). From the spatial distribution of the flyschoid facies, forming the belt bordering the basin's north-eastern margin (Klein *et al*. 1979), it can be inferred that the dominant impulse for the formation of gravity flows was an increased seismicity in the adjacent source areas that were tectonically active since the formation of the Bohemian Cretaceous Basin (Tröger 1969, Valečka 1979, Klein *et al*. 1979, Skoček & Valečka 1983). The seismic activity at the north-eastern margin of the basin is confirmed by structures (extention cracks, circular and elongate collapse structures and fracture zones) and sediments (seismites) produced during seismic events described by Wojewoda (1987). The deposition of the Merboltice Fm. with its rapid sedimentation of dominantly sandy beds from gravity flows represents a dramatic change. The sedimentation was influenced by accelerated uplift of the source area, due to increased movement activity at the Lusatian Fault, which is one of the most important structures in the Elbe Fault System (Scheck *et al*. 2002, Jelínek *et al*. 2020). This Lusatian Fault of Variscan origin was characterized by intense block movements even before the Cretaceous (Coubal *et al*. 2014, 2015). During the existence of the Bohemian Cretaceous Basin, movements on the Lusatian Fault were continuous and the most intense of all faults (see also Geological and tectonic setting). On the Lusatian Fault, structures related to earthquake activity have also been identified, although not dated (Coubal *et al.* 2018). Block vertical movements, often inverse, reached hundreds of metres to more than 1 km. The rapid uplift of the source area led to its accelerated erosion, cut, among others, deep into the unweathered granitoids. The uplift may have been accompanied by a gradient increase of the bottom slope in the adjacent segment of the basin facilitating gravity flows activity. Detritus rapidly accumulated in the nearshore part of the basin and was transported further into the basin by gravity currents. For these reasons, I presume the gravity currents were initiated primarily by seismic activity at the Lusatian Fault. The gravity currents carried detritus in rapidly repeating pulses up to 50 km from the basin margin. The frequency of these pulses made sedimentation of fine-grained muddy sediments deposited from the suspension almost impossible. These were deposited only intermittently, in pauses between the deposition from gravity flows. They are therefore sparse, occurring only in thin layers between some beds (sections 4, 10 in Figs 7, 8). It is generally assumed that gravity flows are triggered not only by earthquakes but also by storms or river floods. Severe storms can increase suspended sediment concentrations near the bottom and trigger gravity flows (Puig *et al.* 2004). Currents induced by these processes might have been active in the formation of Merboltice Fm.

According to Voigt (2011) and Valečka (2019) deposits formed during strong storms occur in the progradation area near the Lusatian Fault in the psammitic Jizera (Postelwitz) and Teplice fms. These deposits are normally graded beds, up to about 1 m thick, with an erosional base. The influence of river floods generating hyperpycnal flows is not documented as the Merboltice Fm. lacks features typical of hyperpycnites – reverse gradation and sharp, erosional boundaries within the beds (Mulder *et al*. 2003). Another factor that could have triggered gravity flows in the Merboltice Fm. is a failure of a thick sand layer, rapidly deposited on the sloping nearshore zone. Rapidly or gradually deposited thick sand layer may have formed at the river mouth as a delta. According to the Bailey *et al.* (2021) rapid or sustained sediment supply can produce elevated pore pressure and thus destabilize the sediment layer. Moderate storm-waves, for example, are then sufficient to collapse the sediment and trigger gravity flows.

Source area, faults activity, climate conditions

The elevated clastic input from the source was compensated by accelerated subsidence of the basin segment adjacent to the very active Lusatian Fault, in the subsided segment the maximum preserved thicknesses of the Cretaceous strata are concentrated (Klein *et al.* 1979, Valečka 1989), with a total value about 1.2 km (Valečka 1979). The absence of analogous Santonian deposits in the North Sudetic Basin can be explained by a weak activity of the Intra-Sudetic and Sudetic Marginal faults, located at the margins of this basin. Similarly, inactive were the West Lusatian and Mid-Saxonian faults, which do not manifest themselves as the boundaries of sedimentary area or in facies development of the Merboltice Fm. (Fig. 16). A possible change of the watershed in the source area that was shifted to its north edge may have played a role in the deposition of the Merboltice Fm., so that the bulk of the detritus was carried into the Bohemian Cretaceous Basin. In the source area, mainly granitoids and older Cretaceous, and to a lesser extent Permian deposits were exposed. The smallest areas were occupied by metamorphites in the cover of the Lusatian granitoid Massif. Sedimentation of Merboltice Fm. took place in climatic conditions similar to those of the South Bohemian Basin. Váchová (2007), Váchová & Kvaček (2009) and Heřmanová *et al*. (2021) assumed a humid seasonally dry paratropical to warm temperate climate, with a mean annual temperature about 15 °C and mean precipitation about 800 mm for these basins. A similar climate, with a mean temperature of about 17 °C and precipitation of 840 mm, was assumed by Kvaček *et al*. (2015) for the underlying flysch-like facies. The existence of plant cover in the source area is evidenced by centimetre- to decimetre-sized fragments of wood and leaves and abundant small fragments of coalified plant matter scattered in the sandstones and forming accumulations in the laminas and abundant in the mudstones near the top of the beds.

Conclusions

(1) The Merboltice Formation consists of a sequence of beds, each up to about 5 m thick. The beds are composed of fine- to medium-grained rarely also coarse-grained subarcoses, mostly gradationally overlain by dark mudstones. Thin, sharp-bounded, light grey to greenish mudstone interbeds occur rarely between these beds.

(2) The beds were deposited by gravity flows. The majority of the beds were deposited in the first phase from a cohesive debris flow that changed into low-density turbidity current by the end of the event. Most of the beds represent cogenetic turbidite-debrite beds. A smaller part of the beds was deposited as single debrites or turbidites. The activity of the gravity flows was made possible by a clay matrix content between 6% and 15%, sporadically up to 17.6%.

(3) Subarcoses contain 70–85% quartz clasts (average 78.5%), 6–15% feldspar clasts (average 8%) and 6–15% clay matrix. Some of the K-feldspars, including microcline, are unaltered or only weakly altered. Among the rock clasts, granitoid clasts, consisting of feldspar and quartz phenocrysts, occur in addition to quartzite and silicite grains.

(4) Merboltice Fm. is almost fossil-free. The available trace fossils cannot be used to interpret water depth as the assemblage contains taxa that were reported from both shallow and deep-water environments (*Ophiomorpha* and *Paleodictyon*, respectively).

(5) Merboltice Fm. was deposited during a significant regressive phase, also documented in the eastern part of the Bohemian Cretaceous Basin and in other Cretaceous basins in the Bohemian Massif, in the North Sudetic Basin and in the Bavarian Basin.

(6) Merboltice Fm., with the dominant influence of gravity flows, represents an anomaly among all sedimentary fills of Cretaceous basins of the Bohemian Massif.

(7) The impulse for gravity flows was mostly related to an intense seismic activity at the Lusatian Fault that probably formed the basin's north-eastern margin in the Santonian. Syndepositional activity of other faults in the Elbe Fault System is not documented from the Merboltice Fm.

Other faults in the Elbe Fault System were seismically inactive. Another factor triggering gravity flows could be storms or a failure of thick sand layers (deltas) at the mouths of rivers attacked by storm waves. Structures indicating the influence of hyperpycnites (river floods) were not detected.

(8) Along the Lusatian Fault, the source area was intensely uplifted, exposing older (mainly Cretaceous) sediments and granitoids of the Lusatian Massif, and to a lesser extent metamorphites. The uplift was accompanied by intense erosion cut even into unweathered granitoids.

Acknowledgements

This research was supported by the Strategic Research Plan of the Czech Geological Survey (DKRVO/ČGS 2023-2027; internal project No. 311430). Zuzana Vařilová from the Municipal Museum in Ústí nad Labem is thanked for the opportunity to study trace fossils from the collections of the museum and J. Preclík for their photographs. Stanislav Čech is thanked for providing the photograph of *Inoceramus* sp. from the Merboltice locality. I am very grateful to the reviewer Jiří Laurin and an anonymous reviewer for their constructive comments which led to improvements of the text and its structure. I thank also Štěpán Manda and Zuzana Tasáryová for editing the article. Technician Lucie Jandová is thanked for the technical processing of the figures.

References

Amy, L.A., Talling, P.J., Peakall, J., Wynn, R.B. & Arzola Thyne, R.G. 2005. Bed geometry used to test recognition criteria of turbidites and (sandy) debrites. *Sedimentary Geology 179*, 163–174. DOI 10.1016/j.sedgeo.2005.04.007

Amy, L.A. & Talling, P.J. 2006. Anatomy of turbidites and linked debrites based on long distance (120 × 30 km) bed correlation, Marnoso Arenacea Formation, Northern Apennines, Italy. *Sedimentology 53*, 161–212. DOI 10.1111/j.1365-3091.2005.00756.x

Andert, H. 1929. Die Kreideablagerungen zwischen Elbe und Jeschken. Teil II. Die nordböhmische Kreide zwischen Elbsandsteingebirge und Jeschken und das Zittauer Sandsteingebirge. *Abhandlungen der Preussischen Geologischen Landesanstalt. Neue Folge, Heft 117*, 1–227.

Andert, H. 1934. Die Kreideablagerungen zwischen Elbe und Jeschken. Teil III. Die Fauna der obersten Kreide in Sachsen, Böhmen und Schlesien. *Abhandlungen der Preussischen Geologischen Landesanstalt. Neue Folge, Heft 159*, 1–477.

Arkhandelsky, A.D. 1912. Upper Cretaceous deposits of the Eastern part of the European Russia. Reprinted in Akademik A.D. Arkhandelsky, *Izobrannye Trudy 1*, 133–466. Izdatelstvo Akademii Nauk SSSR, Moskva. [in Russian]

Bailey, L.P., Clare, M.A., Rosenberger, K.J., Cartigny, M.J.B., Talling, P.J., Paull, C.K., Gwiazda, R., Parsons, D.R., Simmons, S.M., Xu, J., Haigh, I.D., Maier, K.L., McGann, M. & Lundsten, E. 2021. Preconditioning by sediment accumulation can produce powerful turbidity currents without major external triggers. *Earth and Planetary Science Letters 562*, art. 116845. DOI 10.1016/j epsl.2021.116845

Biernacka, J. 2012. Provenance of Upper Cretaceous quartz-rich sandstones from the North Sudetic Synclinorium, SW Poland: constraints from detrital tourmaline. *Geological Quarterly 56*, 315–332. DOI 10.7306/gq.1024

Bouma, A.H. 1962. *Sedimentology of some flysch deposits*. 168 pp. Elsevier, Amsterdam & New York.

Bubík, M., Stráník, Z. & Švábenická, L. 1995. Výskyty svrchnokřídového pálavského souvrství v příležitostných odkryvech ve městě Mikulov. *Geological Research in Moravia and Silesia in the year 1994*, 23–27.

Čech, S., Klein, V., Kříž, J. & Valečka, J. 1980. Revision of the Upper Cretaceous stratigraphy of the Bohemian Cretaceous Basin. *Věstník Ústředního Ústavu Geologického 55*, 277–296.

Coubal, M., Adamovič, J., Málek, J. & Prouza, V. 2014. Architecture of thrust faults with alongstrike variations in fault-plane dip: Anatomy of the Lusatian Fault, Bohemian Massif. *Journal of Geosciences 59*, 183–208. DOI 10.3190/jgeosci.174

Coubal, M., Málek, J., Adamovič, J. & Štěpančíková, P. 2015. Late Cretaceous and Cenozoic dynamics of the Bohemian Massif inferred from the paleostress history of the Lusatian Fault Belt. *Journal of Geodynamics 87*, 26–49. DOI 10.1016/j.jog.2015.02.006

Coubal, M., Adamovič, J. & Šťastný, M. (eds) 2018. *Lužický zlom – hranice mezi dvěma světy.* 272 pp. Novela bohemica, Praha.

Demircan, H. & Uchmann, A. 2017. Short distance variability of trace fossils in submarine slope and proximal basin plain deposits: a case study from the Ceylan Formation (Upper Eocene), Gelibolu Peninsula, NW Turkey. *Bolletino della Società Paleontologica Italiana 56*, 253–275.

Domácí, L. 1976. Continental Paleogene of the Bohemian Massif. *Acta Universitatis Carolinae, Geologica 2*, 135–146.

Dott, R.L. 1964. Wacke, greywacke and matrix – What approach to immature sandstone classification? *Journal of Sedimentary Petrology 34*, 625–632. DOI 10.1306/74D71109-2B21-11D7-8648000102C1865D

Eliáš, M. & Wessely, G. 1990. The autochtonous Mesozoic on the eastern flank of the Bohemian Massif – an object of mutual geological efforts between Austria and ČSSR, 78–83. *In* Minaříková, D. & Lobitzer, H. (eds) *Thirty years of geological cooperation between Austria and Czechoslovakia*. Federal Geological Survey Vienna, Geological Survey Prague.

Folk, R.L. 1954. The distinction between grain-size and mineral composition in sedimentary rock nomenclature. *The Journal of Geology 62*, 344–359. DOI 10.1086/626171

Fürsich, F.T., Taheri, J. & Wilmsen, M. 2007. New occurence of the trace fossil Paleodictyon in shallow marine environments: Examples from Triassic-Jurassic of Iran. *Palaios 22*, 408–416. DOI 10.2110/palo.2006.p06-041r

Gabriel, M. 1984. Deposit of kaolinite sand near Dolní Zálezly. *Časopis pro mineralogii a geologii 29*, 1–18.

Garzanti, E. 2017. The Maturity Myth In Sedimentary and Provenance Analysis. *Journal of Sedimentary Research 87*, 358–365. DOI 10.2110/jsr.2017.17

Garzanti, E. & Ando, S. 2007. Heavy mineral concentration in modern sands. *Developments in Sedimentology 58*, 517–545. DOI 10.1016/S0070-4571(07)58020-9

Grossouvre, A. de 1894. Recherches sur la Craie supérieure. II. Paléontologie. Les ammonites de la Craie superiéure. *Mémoires pour servie a l'éxplication de la carte géologique détaillé de la France 1894*, 1–264. DOI 10.5962/bhl.title.46845

Hampton, M. 1975. Competence of fine-grained debris flows. *Journal of Sedimentary Research 45*, 834–844. DOI 10.1306/212F6E5B-2B24-11D7-8648000102C1865D

Hercogová, J. 1985. *Mikrobiostratigrafie křídy v hlubokých vrtch SG v kladském prolomu*. 10 pp. MS Archive, Czech Geological Survey.

Hercogová, J. & Valečka, J. 1977. Coniac-Ablagerungen in die Kreide Ostböhmens. *Věstník Ústředního ústavu geologického 52*, 371–375.

Herm, D. 1979. Die süddeutsche Kreide – Ein Überblick. Aspekte der Kreide Europas. *IUGS Series A 6*, 85 –106.

Heřmanová, Z., Kvaček, J.D. & Friis, E.M. 2021. Plant mesofossils from the Late Cretaceous Klikov Formation, the Czech Republic. *Fossil Imprint 77*, 256–270. DOI 10.37520/fi.2021.018

Hibsch, J.E. 1924. *Geologische Karte des Böhmischen Mittelgebirges und angrenzenden Gebiete, umfassend die Bezirke Tetschen, Aussig u. Leitmeritz. Maßstab 1:100,000*. Herausgegeben v. Freien Lehreverein für den politische Bezirk Tetschen a.d. Elbe.

Hibsch, J.E. 1927. *Erläuterungen zur geologischen Karte der Umgebung von Böhm. Kamnitz.* 99 pp. Knihovna Státního geologického ústavu Československé republiky, svazek 10, Praha.

Hibsch, J.E. 1930a. Das geologische Alter der bisher für Tertiär gehaltenen Sandablagerungen im Böhmischen Mittelgebirge. *Mineralogische und petrographische Mitteilungen 40*, 67–72. DOI 10.1007/BF02938418

Hibsch, J.E. 1930b. *Erläuterungen zur geologischen Karte der Umgebung von Graber u. Kosel westl. Böhm. Leipa.* 50 pp., Státní geologický ústav Československé republiky, Praha.

Hubert, J.F. 1962. A Zircon-Tourmaline-Rutile Maturity Index and Independence of Composition of Heavy Mineral Assemblages with Gross Composition and Texture of Sandstone. *Journal of Sedimentary Petrology 32*, 440–450. DOI 10.1306/74D70CE5-2B21-11D7-8648000102C1865D

James, W.C., Mack, G.H. & Suttner, L.J. 1981. Relative alteration of microcline and sodic plagioklase in semi-arid and humid climates. *Journal of Sedimentary Petrology 51*, 151–164. DOI 10.1306/212F7C34-2B24-11D7-8648000102C1865D

Jelínek, J., Krentz, O., Mlčoch, B., Nadaskay, R. & Valečka, J. 2020. Tektonik, 33–40. *In* Mrázová, Š., Tomanová Petrová, P. & Krentz, O. (eds) *Geologie des Sächsisch-Böhmischen Kreidebeckens zwischen Erzgebirge und Jeschken.*

JERZYKIEWICZ, T. 1970. The Upper Cretaceous Turbidite Sequence in the Sudetes (South-western Poland). *Bulletin de l'Academie des Sciences, Série des Sciences Géologiques et Géographiques 18*, 149–159.

JERZYKIEWICZ, T. 1971. A flysch/littoral succesion in the Sudetic Upper Cretaceous. *Acta Geologica Polonica 21*, 165–200.

JOHNSSON, M.J. 1993. The system controlling the composition of clastic sediments. *Geological Society of America Special Paper 284*, 1–20. DOI 10.1130/SPE284-p1

KEDZIERSKI, M. 2008. Calcareous nannofossils and inoceramid biostratigraphies of Middle Turonian to Middle Coniacian from the Opole trough of SW Poland. *Cretaceous Research 29*, 451–467. DOI 10.1016/j.cretres.2007.06.004

KLEIN, V. & SOUKUP, J. 1963. Křída, 80–113. *In* HORNÝ, R. (ed.) *Vysvětlivky ke geologické mapě ČSSR 1:200 000. M-33-XV Praha.* Ústřední ústav geologický, Praha.

KLEIN, V., MÜLLER, V. & VALEČKA, J. 1979. Lithofazielle und paläogeographische Entwicklung des Böhmischen Kreidebeckens. Aspekte der Kreide Europas. *IUGS Series A 6*, 435–446.

KOZDRÓJ, W., KRENTZ, O. & OPLETAL, M. (EDS) 2001. *Comments on the Geological map Lausitz-Jizera-Karkonosze (without Cenozoic sediments) 1:100,000*. 64 pp. Geological Surveys of Germany (Saxony), Poland and the Czech Republic, Warsaw.

KREJČÍ, J. 1869. Studien im Gebiete der böhmischen Kreide-Formation. I. Allgemeine und orographische Verhältnisse, sowie Gliederung der Böhmischen Kreide-Formation. *Archiv der naturwissenschaftlichen Landesdurchforschung von Böhmen 1*, 41–179.

KRUMBEIN, W.C. 1941. Measurement and geological significance of shape and roundness of sedimentary particles. *Journal of Sedimentary Petrology 11*, 64–72. DOI 10.1306/D42690F3-2B26-11D7-8648000102C1865D

KVAČEK, J., HALAMSKI, A.T., SVOBODOVÁ, M. & DURSKA, E. 2015. Coniacian flora from the Sudetes (south-western Poland): Palaeoecological and palaeoclimatic interpretation. *Palaeogeography, Palaeoclimatology, Palaeoecology 436*, 178–187. DOI 10.1016/j.palaeo.2015.06.041

LAURIN, J. & ULIČNÝ, D. 2004. Controls on a Shallow-Water Hemipelagic Carbonate System Adjacent to a Siliciclastic Margin: Example from Late Turonian of Central Europe. *Journal of Sedimentary Research 74*, 697–717. DOI 10.1306/020904740697

LAURIN, J., ULIČNÝ, D., WALTHAM, D., TOMAN, P., WARSITZKA, M. & BRADLEY, B.B. 2023. Contrasting response of sea-level change to orbital eccentricity in greenhouse and icehouse climates. *Earth and Planetary Sciences Letters 622*, 1–13. DOI 10.1016/j.epsl.2023.118421

LESZCZYŃSKI, S., CHRASTEK, A., HALAMSKI, A.T., NEMEC, W. & WOJEWODA, J. 2022. Cretaceous of the North Sudetic synclinorium (southwestern Poland): Stratigraphy, origin and economic importance, 141–197. *In* WALASZCZYK, I. & JORDAN, P.T. (eds) *Cretaceous of Poland and adjacent areas. Field trip guides*. 406 pp. Faculty of geology, University Warsaw, Warsaw.

LOWE, D.R. 1982. Sediment gravity flows: II. Depositional models with special reference to high density turbidity currents. *Journal of sedimentary Research 52*, 279–297. DOI 10.1306/212F7F31-2B24-11D7-8648000102C1865D

MACÁK, F. 1966. *Křídový útvar v severozápadních Čechách (svrchní turon až santon)*. 218 pp. Dissertation thesis, MS Archive, Czech Geological Survey.

MACÁK, F. & MÜLLER, V. 1963. Svrchní coniak až santon v křídě Českého středohoří. *Věstník ústředního ústavu geologického 38*, 193–195.

MACÁK, F. & MÜLLER, V. 1968. Stratigrafie a paleogeografie křídového útvaru v sz. Čechách. Stratigraphie und Paläogeographie der Kreideformation in Nordwestböhmen. *Časopis pro mineralogii a geologii 13*, 37–46.

MALGESINI, G., TALLING, P.J., HOGG, A.J., ARMITAGE, D., GOATER, A. & FELLETI, F. 2015. Quantitative Analysis of Submarine-flow Deposit Shape In the Marenoso-Arenacea Formation: What Is the Signature of Hindered Settling From Dense Near-Bed Layers? *Journal of Sedimentary Research 85*, 170–191. DOI 10.2110/jsr.2015.15

MALÝ, K.D., CAJZ, V., ADAMOVIČ, J. & ZACHARIÁŠ, J. 2006. Silicification of quarz arenites overlain by volcanoclastic deposits: an alternative to silcrete formation. *Geologica Carpathica 57*, 461–472.

MARR, J.G., HARFF, P.A., SHANMUGAN, G. & PARKER, G. 2001. Experiments on subaqueous sandy gravity flows: The role of clay and water content in flow dynamics and depositional structures. *GSC Bulletin 113*, 1377–1386. DOI 10.1130/0016-7606(2001)113<1377:EOSSGF>2.0.CO;2

MEYER, M.K.F. 1996. Kreide, 112–125. *In* FREUDENBERGER, W. & SCHWERD, K. (eds) *Erläterungen zur geologischen Karte von Bayern 1: 500 000. 4. neubearbeitete Auflage*. München.

MIDDLETON, G.V. & HAMPTON, M.A. 1973. Sediment gravity flows: mechanisms of flow and deposition, 1–38. *In* MIDDLETON, G.V. & BOUMA, H.A. (eds) *Turbidites and Deep-Water Sedimentation. SEPM Pacific Section, Short course lecture note*s.

MIKULÁŠ, R. & VAŘILOVÁ, Z. 2021. Zkamenělé stopy pod Bukovou horou. *Příspěvky k ústecké vlastivědě 24*, 43–45.

MILEWICZ, J. 1997. *Górna kreda depresji pólnocnosudeckiej (lito- i biostratigrafia, paleogeografia, tektonika oraz uwagi o surowcach).* 58 pp. Prace geologiczno-mineralogiczne LXI, Wydawnictwo Uniwersitetu Wroclavskiego, Wroclaw.

MORTON, A.C. & HALLSWORTH, C.R. 1999. Processes controlling the composition of heavy mineral assemblages in sandstones. *Sedimentary Geology 124*, 3–29. DOI 10.1016/S0037-0738(98)00118-3

MULDER, T. & ALEXANDER, A. 2001. The physical character of subaqueous sedimentary density flows and their deposits. *Sedimentology 48*, 269–299. DOI 10.1046/j.1365-3091.2001.00360.x

MULDER, T., SYVITSKY, J.P.M., MIGEON, S., FAUGERES, J.-C. & SAVOYE, B. 2003. Marine hyperpycnal flows: initiation, behavior and related deposits. A review. *Marine and Petroleum Geology 20*, 861–882. DOI 10.1016/j.marpetgeo.2003.01.003

MÜLLER, G. 1887. Beitrag zur Kenntnis der oberen Kreide am nördlichen Harzrande. *Jahrbuch der Preussischen Geologischen Landesanstalt zu Berlin 8*, 372–456.

Mutti, E. 1992. *Turbidite sandstones.* 275 pp. Agip Special Publication, Milan.

Nádaskay, R., Žák, J., Sláma, J., Sidorinová, T. & Valečka, J. 2019. Deciphering the Late Paleozoic to Mesozoic tectonosedimentary evolution on the northern Bohemian Massif from detrical zircon geochronology and heavy mineral provenance. *International Journal of Earth Sciences 108*, 2653–2681. DOI 10.1007/s00531-019-01781-z

Niebuhr, B., Pürner, T. & Wilmsen, M. 2009. Litho- und Biostratigraphie der außeralpinen Kreide von Bayern. Beitrag zur Stratigraphie von Deutschland im Auftrag der Deutschen Stratigraphischen Kommission. *Schriftenreihe der Deutschen Gesselschaft für Geowissenschaften 65*, 7–58.

Opletal, M. & Prouza, V. 2006. Paleozoikum, 11–15. *In* Opletal, M. et al. (eds) *Vysvětlivky k základní geologické mapě České republiky 1:25 000, 02-214 Dolní Poustevna, 02-223 Mikulášovice*. 57 pp. Czech Geological Survey, Prague.

Pettijohn, F.J., Potter, P.E. & Siever, R. 1972. *Sand and sandstone, 2nd edition*. 618 pp. Berlin, Heidelberg & New York. DOI 10.1007/978-1-4615-9974-6

Prinz, K. 1930. Die Kreide-Unterlage des böhmischen Mittelgebirges. *Firgenwald 3*, 110 –116.

Puig, P., Ogston, A.S., Mullenbach, B.L., Nittrouer, C.A., Parsons, J.D. & Sternberg, R.W. 2004. Storm-induced gravity flows at the head of the Eel submarine canyon, northern California margin. *Journal of Geophysical Research 109*, CO3019. DOI 10.1029/2003JC001918

Řehánek, J. 1978. Mikrofacie a mikrofauna (incertae sedis) písčito-glaukonitové série svrchní křídy z podloží karpatské předhlubně a vnějšího flyšového pásma na jižní Moravě. *Zemný plyn a nafta 23*, 313–346.

Scheck, M., Bayer, U., Volker, O., Lamarche, J., Banka, D. & Pharaoh, T. 2002. The Elbe Fault system in North Central Europe – a basement controlled zone of crustal weakness. *Tectonophysics 360*, 281–299.
DOI 10.1016/S0040-1951(02)00357-8

Schlüter, C. 1887. Einige Inoceramen und Cephalopoden der texanischen Kreide: Verhandlungen des Naturhistorischen Vereines der Preussischen Rheinlande. *Westfalens und des Reg.-Bezirks Osnabruck 44th year*, 42–45.

Seilacher, A. 2007. *Trace Fossils Analysis*. 226 pp. Springer Berlin, Heidelberg & New York.

Seitz, O. 1970. Über einige Inoceramen aus der Oberen Kreide. 1. Die Gruppe des Inoceramus subquadratus Schlüter und der Grenzbereich Coniac/Santon. *Beihefte zum Geologischen Jahrbuch 86*, 3–103.

Shanmugam, G. 1996. High-density turbidity currents: are they sandy debris flows? *Journal of Sedimentary Research 66*, 2–10.
DOI 10.1306/D426828E-2B26-11D7-8648000102C1865D

Shanmugam, G. 1997. The Bouma Sequence and the turbidite mind set. *Earth-Science Reviews 42*, 201–229.
DOI 10.1016/S0012-8252(97)81858-2

Shanmugam, G. 2000. 50 years of the turbidite paradigm (1950s–1990s): deep-water processes and facies models – a critical perspective. *Marine and Petroleum Geology 17*, 285–342. DOI 10.1016/S0264-8172(99)00011-2

Shanmugam, G. 2002. Ten turbidite myths. *Earth-Science Review 58*, 311–341. DOI 10.1016/S0012-8252(02)00065-X

Skoček, V. & Valečka, J. 1983. Paleogeography of the Late Cretaceous Quadersandstein of Central Europe. *Palaeogeography, Palaeoclimatology, Palaeoecology 44*, 71–92. DOI 10.1016/0031-0182(83)90005-6

Slánská, J. 1974. Continental Cretaceous and Tertiary sedimentation in the South Bohemian Basin. *Neues Jahrbuch für Geologie und Paläontologie, Abhandlungen 146(3)*, 385–406.

Slavík, J. 1988. Vztah charakteru těžkých minerálů k typu zdrojových oblastí sedimentů na litostratotypové lokalitě Merboltice u Děčína (merboltické souvrství: santon). *Zprávy o geologických výzkumech za rok 1985*, 178–180.

Soukup, J. 1956. Výskyt inoceramů ze skupiny subcardissoides v české křídě. *Sborník ústředního ústavu geologického, oddíl paleontologický 22*, 1–20.

Soukup, J. 1963. Křídový útvar, 43–74. *In* Kopecký, L. (ed.) *Vysvětlivky ke geologické mapě ČSSR 1:200 000 M-33-IX Děčín*. Ústřední ústav geologický, Praha.

Soukup, J. 1968. Chlomek Formation (Chlomecké vrstvy), 75–81. *In* Chlupáč, I. (ed.) *Lexique stratigraphique international. Volume I. Massif de Bohème*. Centre National de la Recherche Scientifique, Paris.

Stráník, Z., Bubík, M., Čech, S. & Švábenická L. 1996. The Upper Cretaceous in south Moravia. *Věstník Českého geologického ústavu 71*, 1–30.

Švábenická, L., Kycl, P. & Rapprich, V. 2016. Stratigraficky nejmladší nanofosílie v sedimentech české křídové pánve. *Zprávy o geologických výzkumech 49*, 19–25.

Svobodová, A., Košťák, M., Čech, S. & Švábenická, L. 2014. New biostratigraphic evidence (texanitid ammonites, inoceramids and calcareous nannofossils) for the Upper and the uppermost Coniacian in the Bohemian Cretaceous Basin. *Zeitschrift der Deutschen Gesellschaft für Geowissenchaften 165*, 577–589. DOI 10.1127/zdgg/2014/0023

Talling, P.J., Amy, L.A. & Wynn, R.B. 2007. New insight into the evolution of large-volume turbidity currents: comparison of turbidite shape and previous modelling results. *Sedimentology 54*, 737–769.
DOI 10.1111/j.1365-3091.2007.00858.x

Talling, P.J., Douglas, G.M., Summer, E.J. & Malgesini, G. 2012. Subaqueous sediment density flows: Depositional processes and deposit types. *Sedimentology 59*, 1937–2003. DOI 10.1111/j.1365-3091.2012.01353.x

Talling, P.J., Malgesini, G. & Feletti, F. 2013. Can liquefied debris flows deposit clean sand over large areas of sea floor? Field evidence from the Maronoso-arenacea Formation, Italian Apennines. *Sedimentology 60*, 720–762.
DOI 10.1111/j.1365-3091.2012.01358.x

Tilmann, H. 1964. Kreide, 141–161. *In* Bayerisches Geologisches Landesamt (ed.) *Erläuterungen zur Geologischen Karte von Bayern 1: 500 000 2. Auflage*.

Tröger, K.A. 1967. Zur Päleontologie, Biostratigraphie und faziellen Ausbildung der unteren Oberkriede (Cenoman bis

Turon), Teil I. *Abhandlungen des Staatlichen Museums der Mineralogie und Geologie zu Dresden 13*, 13 – 207.

Tröger, K.A. 1969. Zur Palaöntologie, Biostratigraphie und faziellen Ausbildung der unteren Oberkreide (Cenoman bis Turon), Teil II. *Abhandlungen des Staatlichen Museum für Mineralogie und Geologie zu Dresden 13*, 1–70.

Uličný, D. 2001. Depositional systems and sequence stratigraphy of coarse-grained deltas in shallow-marine, strike-slip settings: The Bohemian Cretaceous Basin, Czech Republic. *Sedimentology 48*, 599–628. DOI 10.1046/j.1365-3091.2001.00381.x

Uličný, D., Laurin, J. & Čech, S. 2009. Controls on clastic sequence geometries in shallow-transtensional basin: The Bohemian Cretaceous Basin, Czech Republic. *Sedimentology 56*, 1077–1114. DOI 10.1111/j.1365-3091.2008.01021.x

Unger, H.J. & Meyer, M.K.F. 1996. Kreide im Untergrund des Molassebeckens (Purbeck bis Campan), 125–128. *In* Freudenberger, W. & Schwerd, K. (eds) *Erläterungen zur geologischen Karte von Bayern 1:500 000. 4. neubearbeitete Auflage*. München.

Unger, H.J. & Risch, H. 1991. Die thermalwasserbohrung Straubing Th-1 und ihr geologischer Rahmen. *Geologisches Jahrbuch Rundschau A130*, 3–51.

Váchová, Z. 2007. *Paleoklimatologická analýza křídové flóry z jihočeských pánví*. 65 pp. Master thesis, Charles University in Prague, Czech Republic.

Váchová, Z. & Kvaček, J. 2009. Palaeoclimate analysis of the flora of the Klikov Formation, Upper Cretaceous, Czech Republic. *Bulletin of Geosciences 84*, 257–268. DOI 10.3140/bull.geosci.1100

Valečka, J. 1979. Paleogeografie a litofaciální vývoj v severozápadní části české křídové pánve. *Sborník geologických věd, Geologie 33*, 47–81.

Valečka, J. 1984. Storm-surge versus turbidite origin of the Coniacian to Santonian sediments in the eastern part of the Bohemian Cretaceous Basin. *Geologische Rundschau 73*, 651–682. DOI 10.1007/BF01824976

Valečka, J. 1988. Sedimentologie svrchní křídy v králickém příkopu. *Sborník geologických věd, Geologie 43*, 147–191.

Valečka, J. 1989. Sedimentology, stratigraphy and cyclicity of the Jizera Formation (Middle-Upper Turonian) in the Děčín area (N Bohemia). *Věstník Ústředního ústavu geologického 64*, 77–90.

Valečka, J. 1999. Relikt paleogenních pískovců u Benešova nad Ploučnicí. *Zprávy o geologických výzkumech v roce 1998*, 78–81.

Valečka, J. 2019. Jurassic pebbles in the Cretaceous sandstones of the Bohemian Basin as a possible tool for reconstruction of the Late Jurassic and Late Cretaceous palaeogeography. *Volumina Jurassica 17*, 17–38.

Valečka, J. 2020. Transgresní příbřežní vápence korycanských vrstev (cenoman) v centrální části české křídové pánve a diskuse týkající se vzniku této pánve. *Geoscience Research Reports 53*, 149–159.

Valečka, J. & Rejchrt, M. 1973. Litologie a geneze tzv. flyšoidní facie ve v. části Českého středohoří. *Časopis pro mineralogii a geologii 18*, 379–391.

Valečka, J. & Skoček, V. 1991. Late Cretaceous lithoevents in the Bohemian Cretaceous Basin, Czechoslovakia. *Cretaceous Research 12*, 561–577. DOI 10.1016/0195-6671(91)90031-7

Valečka, J. & Slavík, J. 1985. *Litologický a sedimentologický výzkum na křídových stratotypových lokalitách Sutiny a Merboltice*. 31 pp. MS Archives Czech geological Survey.

Valečka, J. & Valigurský, L. 2003. Rozptýlené valouny, slepence a křemence při jihovýchodním okraji Českého středohoří. *Zprávy o geologických výzkumech za rok 2002*, 42–44.

Váně, M. 2001. Geologické postavení skalicko-žitenických eocenních křemenců u Litoměřic. *Sborník severočeského muzea, Přírodní vědy 22*, 3–6.

Voigt, T. 2009. Die Lausitz-Riesengebirgs-Antiklinalzone als kreidezeitliche Inversionsstruktur: Geologische Hinweise aus den umgebenden Kreidebecken. *Zeitschrift für geologische Wissenschaften 37*, 1–39.

Voigt, T. 2011. Sturmdominierte Sedimentation in der Postelwitz Formation (Mittel-Turon) der Sächsischen Kreide. *Freiberger Forschungshefte C 540*, 3–25.

Voigt, S., Wagreich, M., Surlyk, F., Walaszczyk, I., Uličný, D., Čech, S., Voigt, T., Wiese, F., Wilmsen, M., Niebuhr, B., Reich, M., Funk, H., Michalík, J., Jagt, J.W.M., Felder, P.J. & Schulp, A.S. 2008. Cretaceous, 923–997. *In* McCann, T. (ed.) *The Geology of Central Europe. Vol. 2*. DOI 10.1144/CEV2P.3

Voigt, T., Kley, J. & Voigt, S. 2021. Dawn and dusk of Late Cretaceous basin inversion in central Europe. *Solid Earth 12*, 1443–1471. DOI 10.5194/se-12-1443-2021

Walaszczyk, I. 1992. Turonian trough Santonian deposits of the Central Polish Uplands: their facies development, inoceramid paleontology and stratigraphy. *Acta Geologica Polonica 42*, 1–122.

Wegner, T.R. 1905. Die Granulatenkreide des Westlichen Münsterlandes. *Zeitschrift der Deutschen Geologischen Gesselltschaft*, 112–232. DOI 10.1127/zdgg/57/1905/112

Wojewoda, J. 1987. Sejsmotektoniczne osady i struktury w kredowych piaskowcach niecki śródsudeckiej. *Przeglad geologiczny 4*, 169–175.

Wojewoda, J. 1997. Upper Cretaceous littoral- to shelf-sedimentation in the Intrasudetic Basin and Nysa trough, Sudety Mts., 81–96. *In* Wojewoda, J. (ed.) *Obszary Źródlowe: Zapis w Osadach.*

Wojewoda, J., Chrzastek, A. & Sokalski, D. 2022. Late Cretaceous geodynamics in the Middle Sudetes area (sedimentary and ichnological record), 199–248. *In* Walaszczyk, I. & Jordan, P.T. (eds) *Cretaceous of Poland and adjacent areas. Field trip guides*.

Zahálka, Č. 1914. *Útvar křídový v Českém Středohoří*. 465 pp. Čeněk Zahálka, Roudnice.

Zelenka, P. 1980. Santonské pískovce na Ústecku. *Zprávy a studie Krajského muzea v Teplicích 14*, 21–28.